

# The Quest for TROPOMI-Observed En-Route Aviation $\text{NO}_x$ Emissions

Liesbeth Wijn

Delft University of Technology



# The Quest for TROPOMI-Observed En-Route Aviation NO<sub>x</sub> Emissions

by

Liesbeth Wijn

to obtain the degree of Master of Science  
at the Delft University of Technology,  
to be defended publicly on Thursday February 23<sup>rd</sup>, 2023 at 10:00 AM.

Student number: 4567080  
Thesis committee: F. Domingos de Azevedo Quadros, MSc, TU Delft, supervisor  
Dr. I.C. Dedoussi, TU Delft, supervisor  
Prof. dr. ir. M. Snellen, TU Delft  
Dr. D.M. Stam, TU Delft

Cover: © European Space Agency, May 2014

An electronic version of this thesis is available at <http://repository.tudelft.nl/>.

# Preface

This report is the final product of my thesis work and (hopefully) concludes my student life at the faculty of Aerospace Engineering at Delft University. I started my masters as an Air Transport Operations student, focusing on economic efficiency of air travel. However, during my studies my interest has shifted more and more towards environmentally-efficient air travel, such that I was delighted to be able to perform my thesis work in the Aircraft Noise and Climate Effects department of our faculty. I titled this work 'The Quest for TROPOMI-Observed En-Route Aviation NO<sub>x</sub> Emissions' as it has truly felt like a quest: a long search for something that is difficult to find. My quest has unfortunately ended without finding TROPOMI-observed en-route aviation emissions, however, it has been a joy to embark on this quest exploring the potential of TROPOMI and the working of the atmosphere around us. Hopefully, this work can ease research endeavours for future questers.

I would like to thank Irene and Flávio for their supervision and valuable advice throughout this thesis work. Your input, feedback and support have helped me become a better engineer and gave me confidence to continue my quest to its end. I would further like to thank Pepijn Veeffkind for sharing his expertise on the TROPOMI instrument during our meetings. I would also like to thank Bar, Kris, Died, Died, Suuz, Jo and especially Job, Pap and Mam for their continuous support and for still letting me feel smart when my efforts seemed to lead to nothing at all.

*Liesbeth Wijn  
Delft, February 2023*



# Summary

Nitrogen oxide emissions alter the composition of the Earth's atmosphere. Excessive emissions of nitrogen oxides ( $\text{NO}_x \equiv \text{NO} + \text{NO}_2$ ) lead to deterioration of air quality. The effects on air quality are not confined to the local region of emission but may via upper tropospheric long-range transport impact human and ecological health in vast regions around the world. In the upper troposphere itself, en-route aviation forms a major source of  $\text{NO}_x$ , contributing significantly to air quality degradation and thought to cause thousands of premature mortalities annually. As the aviation sector continues to grow,  $\text{NO}_x$  emissions from en-route aviation are also expected to increase. In order to counteract further air quality degradation from en-route aviation, a thorough understanding and documentation of actual emissions is required. Currently, en-route aviation emissions quantification efforts are largely model-based as limited measurement capabilities have been available to quantify actual upper tropospheric nitrogen oxide emissions. Since the launch of satellites capable of remote sensing of the global troposphere, new opportunities for upper tropospheric nitrogen dioxide analysis have emerged.

In this report, a first assessment of the use of TROPOMI, the highest precision remote sensing instrument currently available for  $\text{NO}_2$  measurements, for the detection of en-route aviation  $\text{NO}_x$  is performed. Analysis of aviation intensity, quality of satellite retrievals, and emission estimates from non-aviation anthropogenic sources showed that the North Atlantic, including the North Atlantic Flight Corridor, could have the highest detection potential. Over this corridor, emissions from telemetric observed aircraft are computed considering no advection or dilution and leading to an upper bound for the average accumulation of emissions for the months of April 2020 and April 2021. These emissions are compared with TROPOMI  $\text{NO}_2$  observations retrieved over all sky and cloudy sky scenes. In order to reduce advection influences TROPOMI measurements at locations of aviation observations close to the overpass time are analysed separately.

Results of this assessment show limited potential for detection of en-route aviation emissions by means of TROPOMI observations. The maximum  $\text{NO}_x$  emissions attributable to en-route aviation during April 2020 and April 2021 were found to be lower than detection limits associated with TROPOMI for  $\text{NO}_2$  retrieval. Neither did inspection of TROPOMI measurements at locations of recent aircraft observations retrieve any evidence of aviation-attributable emissions. Apart from the limited expected aviation emissions, detection may be complicated by influences from long-range transport and meteorology as well as uncertainties in the retrieval algorithm of TROPOMI.

General conclusions drawn indicate that the highest precision remote sensing instrument TROPOMI is currently not capable of detecting evidence of en-route aviation emissions over the North Atlantic Flight Corridor during the months of April 2020 and April 2021. Even though the conclusion of this first study does not show optimistic results, recommendations are given for future research into relations between TROPOMI observations and estimated en-route emissions. This research comprised of analysis of the North Atlantic Flight Corridor during two months in which aviation intensity was limited by restrictions to reduce the spread of COVID-19. Therefore, expanding the research window to include months unaffected by COVID-19 restrictions may yield more promising and robust results. Furthermore, the research presented here suggests that meteorology may have large influences on local and regional  $\text{NO}_2$  concentrations. Future researchers are therefore recommended to include meteorology decoupling measures in comparisons. Lastly, efforts into the creation of aviation specific air mass factors for satellite  $\text{NO}_2$  retrieval are encouraged as these may increase the detection likelihood of en-route aviation emissions. The quest shall continue.

# Contents

<b>Preface</b>	<b>i</b>
<b>Summary</b>	<b>ii</b>
<b>List of Figures</b>	<b>iii</b>
<b>Nomenclature</b>	<b>vi</b>
<b>1 Introduction</b>	<b>1</b>
1.1 Motivation . . . . .	1
1.2 Research objective and questions . . . . .	2
1.3 Outline . . . . .	2
<b>2 Research article</b>	<b>4</b>
<b>Assessment of TROPOMI NO<sub>2</sub> observations for detection of en-route aviation NO<sub>x</sub> emissions</b>	
<b>3 Conclusion and recommendations</b>	<b>14</b>
<b>4 Supplements</b>	<b>16</b>
4.1 Location . . . . .	16
4.2 Cloud fraction . . . . .	18
4.3 Air Mass Factor . . . . .	18
4.4 Resolution . . . . .	20
4.5 NO <sub>x</sub> plume age and mixing ratios . . . . .	21
4.6 Meteorology . . . . .	22
<b>Bibliography</b>	<b>24</b>

# List of Figures

2.1	Differences in original geodesic trajectories and adapted trajectories through observation median. . . . .	7
2.2	Example of an averaging kernel for a pixel with an optically thick cloud and averaging kernels for cloud free pixels with varying surface albedo (Eskes and Boersma [2003]). . . . .	7
3.3	Zonally averaged measured $\text{NO}_2$ vertical column densities over the eastern North Atlantic (East of $35^\circ$ W) and expected peaks from openAVEM as function of latitude. . . . .	8
3.1	Average openAVEM expected $\text{NO}_x$ vertical column densities over the North Atlantic during April 2020 (left) and April 2021 (right). . . . .	9
3.2	Average TROPOMI measured $\text{NO}_2$ vertical column densities over the North Atlantic during April 2020 (left) and April 2021 (right). . . . .	9
3.4	Zonally averaged year-on-year increases in measured $\text{NO}_2$ vertical column densities over the eastern North Atlantic (East of $35^\circ$ W) and expected increases in $\text{NO}_x$ from openAVEM as function of latitude. . . . .	9
3.5	Monthly averaged expected $\text{NO}_x$ from en-route aviation and TROPOMI measurement precision per $0.05^\circ$ grid cell. Inset values display medians. . . . .	9
3.6	Precision of cloudy and clear sky measurements. . . . .	10
3.7	Comparison of monthly $\text{NO}_2$ measurements over all and cloudy only scenes over the North Atlantic. . . . .	10
3.8	Average TROPOMI measured $\text{NO}_2$ vertical column densities over the North Atlantic over cloudy scenes during April 2020 and April 2021. . . . .	10
3.9	Zonally averaged cloudy measured $\text{NO}_2$ vertical column densities over the eastern North Atlantic (East of $35^\circ$ W) and expected peaks from openAVEM as function of latitude. . . . .	11
3.10	Zonally averaged year-on-year increases in measured $\text{NO}_2$ vertical column densities over the cloudy scenes over the eastern North Atlantic (East of $35^\circ$ W) and expected increases from openAVEM as function of latitude. . . . .	11
3.11	Comparison of TROPOMI $\text{NO}_2$ downwind minus upwind measurements at locations of recent aviation activity with openAVEM expectations. . . . .	11
4.1	Average quality assurance value of TROPOMI measurements. . . . .	16
4.2	Aviation intensity during the least flown week. . . . .	17
4.3	Aviation intensity during the most flown week. . . . .	17
4.4	Average rate of non-aviation anthropogenic emissions during April 2019. . . . .	17
4.5	Example of a stripe (from $38^\circ$ W, $40^\circ$ N towards the upper left ( $41^\circ$ W, $52^\circ$ N) created by pixel dependent offsets that may be confused with en-route aircraft emissions . . . . .	17
4.6	Increase in available days for analysis when relaxing the cloud fraction condition from 1.0 to $\geq 0.75$ . . . . .	18
4.7	Comparison of $\text{NO}_2$ VCD measurements over fully ( $\text{CF} = 1$ ) and partly ( $\text{CF} \geq 0.75$ ) cloudy scenes . . . . .	18
4.8	Average TROPOMI retrievals when considering $\text{CF}=1$ . . . . .	18
4.9	Visualisation of separation of geometric and detailed AMFs per atmospheric section . . . . .	19
4.10	Absolute difference in average geometric and TROPOMI AMF computed VCDs over the NAFC . . . . .	19
4.11	Difference in average geometric and TROPOMI AMF computed VCDs over the NAFC . . . . .	19
4.12	Average $\text{AMF}_{geo,trop}$ -retrieved TROPOMI $\text{NO}_2$ VCDs over the NAFC . . . . .	20
4.13	Difference in $\text{NO}_2$ VCDs when applying a geometric kernel to both the stratospheric and tropospheric contribution and when applying it solely to the tropospheric contribution . . . . .	20
4.14	A plume-like structures in the retrieved TROPOMI $\text{NO}_2$ VCDs can for example be observed between the aircraft observations at ( $53^\circ$ W, $49.5^\circ$ N) and ( $50.5^\circ$ W, $49.75^\circ$ N) . . . . .	21
4.15	Persisting plume-like structures in $\text{AMF}_{geo}$ -retrieved $\text{NO}_2$ VCDs near aircraft observations over the same scene . . . . .	21
4.16	Cloudiness over the scene in which the plume-like structures are observed . . . . .	21

---

4.17 Average April 2021 emission estimates from openAVEM when considering a 3 hour plume age . . . . .	22
4.18 Absolute difference in expected emissions when decreasing plume age from 10 to 3 hours	22
4.19 Emission estimates when considering the reported NO <sub>2</sub> /NO <sub>x</sub> -ratio of 0.42 . . . . .	22
4.20 Average meteo-attributable contribution of measured NO <sub>2</sub> VCDs . . . . .	23

# Nomenclature

## Acronyms

Acronym	Definition
ADS-B	Automatic Dependent Surveillance-Broadcast
openAVEM	Open Aviation Emission Model
AMF	Air Mass Factor
BADA	Base of Aircraft Data
CEDS	Community Emissions Data System
COVID-19	Corona Virus Disease 2019
DOAS	Differential Optical Absorption Spectroscopy
ESA	European Space Agency
FRESCO-S	Fast Retrieval Scheme for Clouds from the Oxygen A-band
GOME	Global Ozone Monitoring Experiment
IATA	International Air Transport Association
ICAO	International Civil Aviation Organisation
LTO	Landing and Take-Off
MERRA-2	Second Modern Era Retrospective Analysis for Research and Applications
NA	North Atlantic (in this research the box between (60° W - 10° W, 40° N - 65° N))
NAFC	North Atlantic Flight Corridor
NAO	North Atlantic Oscillation
NIR	Near Infrared Light
OMI	Ozone Monitoring Instrument
TROPOMI	Tropospheric Monitoring Instrument
UV-VIS	Ultraviolet and Visible Light
VCD	Vertical Column Density

## Symbols

Symbol	Definition	
HNO <sub>3</sub>	Nitric acid	
NO	Nitric oxide	
NO <sub>x</sub>	Nitrogen oxides	
NO <sub>2</sub>	Nitrogen dioxide	
N <sub>2</sub> O <sub>5</sub>	Dinitrogenpentoxide	
O <sub>3</sub>	Ozone	
$SCD_{trop}$	Slant column density of the troposphere	[ $Pmolec/cm^2$ ]
$SZA$	Solar zenith angle	radians
$VCD_{tot}$	Summed vertical column density of the troposphere and stratosphere	[ $Pmolec/cm^2$ ]
$VCD_{trop}$	Tropospheric vertical column density	[ $Pmolec/cm^2$ ]
$VCD_{strat}$	Stratospheric vertical column density	[ $Pmolec/cm^2$ ]
$VZA$	Viewing zenith angle	radians
$\mu$	Mean	
$\sigma$	Standard deviation	

# Introduction

This chapter introduces the thesis work. First, the motivation for this research is highlighted in section 1.1. Subsequently, the research objective and main research questions are defined in section 1.2. Finally, the structure of this report is given in section 1.3.

## 1.1. Motivation

Nitrogen oxides are essential elements in the atmosphere. However, excessive levels of nitrogen oxides and their successors can impact the air quality threatening human and ecological health. Nitrogen oxide induced degradation of air quality (Masiol and Harrison [2014]) can induce respiratory and cardiovascular diseases in humans leading to premature mortalities (Lelieveld et al. [2015], Kampa and Castanas [2008]), and lead to declines in biodiversity and total biological population (HCON [2004], Manisalidis et al. [2020]). Since the industrial revolution, emissions of nitrogen oxides from anthropogenic sources including the aviation sector have increased atmospheric levels of nitrogen dioxide drastically (Hoesly et al. [2018]).

The effects of air pollution such as those caused by aviation are not confined to the region of emissions (Fowler et al. [2020]) and may instead include the free troposphere leading to premature mortalities on a global scale (Lelieveld et al. [2015]). In the upper troposphere, emissions from en-route aviation form a primary source of  $\text{NO}_x$ , contributing to air quality degradation (Masiol and Harrison [2014], Grobler et al. [2019], Tarrasón et al. [2004], Cameron et al. [2017]) and cause for 8.000-12.000 premature deaths annually (Barrett et al. [2010], Yim et al. [2015]).

Even with more stringent aviation emission regulations, advances in engine technology and more efficient air traffic control,  $\text{NO}_x$  emissions from aircraft are expected to grow by 55% to 143% until 2050, depending on the forecasted growth in air traffic (Quadros et al. [2022a]). The severe consequences of en-route aviation  $\text{NO}_x$  emissions on human and ecological health and their expected growth, require thorough understanding and documentation of en-route aviation emissions.

Studies into en-route aviation emissions have, however, been heavily model-based (Tarrasón et al. [2004], Barrett et al. [2010], Lee et al. [2013], Jacobson et al. [2013], and Morita et al. [2014]) as limited measurement capability has been available for upper tropospheric and lower stratospheric nitrogen dioxide. The recent launch of remote sensing instruments on satellites has opened new opportunities for upper tropospheric research and the role of aviation emissions therein.

The most recently launched Sentinel 5-Precursor satellite TROPOMI is capable of sensing a wide wavelength spectrum (400 - 2600 nm) at high spatial resolution (3.5 km by 5.5 km since August 2019) enabling high quality measurements of a large variation of species (Veefkind et al. [2012]). Advances in aviation surveillance technology by satellites have further increased research potential to observe actual en-route aviation emissions directly from space. Recent investigations into upper tropospheric nitrogen dioxide concentrations (Marais et al. [2021]) and lightning  $\text{NO}_x$  emissions (Pérez-Invernón et al. [2022], Bucsela et al. [2021], Allen et al. [2021]) have successfully used the cloud retrieval algorithm of TROPOMI to compute upper tropospheric nitrogen dioxide mixing ratios and help detect lightning  $\text{NO}_x$  emissions. As en-route aviation emissions are likewise emitted in the upper troposphere, the cloud retrieval algorithm could be of advantage.

In this thesis work is investigated to what extent modelled nitrogen oxide emissions can be related

to (cloudy) satellite observations such that a first step towards documentation of actual global cruise level  $\text{NO}_x$  emissions can be undertaken.

## 1.2. Research objective and questions

As has become evident, it is of importance to document  $\text{NO}_x$  emissions along all stages of flight, to accurately denote the impact of aviation on climate and air quality and develop measures to mitigate the impact on regional and global scale. Especially during the non-LTO (non-Landing and Take-Off) phases of flight, detection and documentation of actual  $\text{NO}_x$  emissions has been challenging. In this research is investigated whether remote sensing spectrometers can aid in this challenge. Therefore, the objective of this research has been formulated as follows:

**Research objective:** *To analyse the possibility of using satellite remote sensing for the detection of en-route aviation emissions by determining to what extent relations exist between en-route aviation activity and satellite observed  $\text{NO}_2$  concentration levels when comparing aircraft  $\text{NO}_x$  emission estimates with TROPOMI measurements.*

### Research questions

Aviation observation data that has been available to conduct this research comprises the months of April 2020 and April 2021. These months were initially selected with the prospect of relating spatio-temporal trends in TROPOMI  $\text{NO}_2$  observations and air traffic intensity. During April 2020, aviation intensity was limited due to COVID-19 induced lockdown regulations, such that changes in  $\text{NO}_x$  emissions were expected compared to emissions in April 2021. As it is unknown whether  $\text{NO}_x$  emissions of aviation are at all observable during these months, this is first investigated in this thesis. Therefore, the main research question that must be answered to reach the objective has been composed as follows:

**Main:** *To what extent do relations exist between estimates of  $\text{NO}_x$  emissions from aviation activity and  $\text{NO}_2$  concentration levels as observed by TROPOMI measurements during April 2020 and April 2021?*

To answer the main research question, a division into sub-questions is performed.

**RQ A:** *In what circumstances are aviation-attributable patterns most likely to be detected in  $\text{NO}_x$  emission estimates and TROPOMI observations of  $\text{NO}_2$  concentration levels April 2020 and April 2021?* This can be identified by researching the following aspects:

- a.i) Aviation intensity
- a.ii) Non-aviation sources of nitrogen oxides
- a.iii) Quality of satellite observation
- a.iv) Cloudiness

**RQ B:** *To what extent can patterns in monthly  $\text{NO}_x$  emissions be observed in satellite retrieved  $\text{NO}_2$  concentration levels?*

- b.i) Spatial distributions of monthly estimates of aviation  $\text{NO}_x$  emissions
- b.ii) Spatial distributions of monthly  $\text{NO}_2$  concentration measurements
- b.iii) Meteorological influences

**RQ C:** *To what extent can  $\text{NO}_x$  contributions of recent aircraft plumes be observed in satellite retrieved  $\text{NO}_2$  concentration levels?*

- c.i) Distribution of estimated recent  $\text{NO}_x$  emissions
- c.ii) Distribution of observed  $\text{NO}_2$  concentration levels
- c.iii) Advection influences

## 1.3. Outline

The research objective outlined in section 1.2 will be addressed in Chapter 2. Chapter 2 is structured as article and begins with another abstract and introduction in Section 1, which does contain some

---

inevitable overlap with those of the complete report. Thereafter, an overview of the materials and methods that are used are presented in Section 2. In Section 3, the results of the comparisons of clear sky and cloudy TROPOMI measurements with emission estimates are presented and discussed. Finally, the article is closed with concluding remarks in Section 4. The thesis report continues after the article with the conclusions and recommendations in Chapter 3 in which, among others, the research questions will be answered and suggestions will be made for future research with the aim of detecting en-route aviation emissions. For conciseness reasons, in the article, some parts of the research are not treated in detail. The interested reader will be directed to more descriptive work in Chapter 4.



# Assessment of TROPOMI NO<sub>2</sub> observations for detection of en-route aviation NO<sub>x</sub> emissions

---

## Abstract

In this work the possibility for use of the satellite remote sensing instrument TROPOMI to detect NO<sub>x</sub> emissions from en-route aviation is assessed. Analysis of aviation intensity, quality of satellite retrievals, and emissions from non-aviation anthropogenic sources showed that the North Atlantic, including the North Atlantic Flight Corridor, could have high detection potential. Over this corridor, emissions from telemetric observed aircraft are computed under assumption of stable meteorology leading to an upper bound for the average accumulation of emissions for the months of April 2020 and April 2021. These emissions are compared with TROPOMI NO<sub>2</sub> observations retrieved over all sky and cloudy sky scenes. In order to reduce advection influences, TROPOMI measurements at locations of aviation observations close to the overpass time are analysed separately.

General conclusions of this first assessment are not optimistic for detection of en-route aviation emissions by means of TROPOMI observations. The maximum NO<sub>x</sub> emissions attributable to en-route aviation over the North Atlantic Flight Corridor during April 2020 and April 2021 were found to be lower than detection limits associated with TROPOMI for NO<sub>2</sub> retrieval. Neither did inspection of TROPOMI measurements at locations of recent aircraft observations retrieve any evidence of aviation-attributable emissions. Therefore detection, documentation and quantification of actual NO<sub>x</sub> emissions from en-route aviation remains a challenge.

---

## 1. Introduction

Nitrogen oxide emissions alter the composition of the atmosphere. Excessive emissions of nitrogen oxides (NO<sub>x</sub> ≡ NO + NO<sub>2</sub>) lead to a deterioration of air quality (Masiol and Harrison [2014]). The effects on air quality are not confined to the local region of emission but may via upper tropospheric long-range transport impact human and ecological health in vast regions around the world (Donnelly et al. [2015], Lelieveld et al. [2015], Manisalidis et al. [2020]). In the upper troposphere itself, en-route aviation forms a primary source of NO<sub>x</sub>,

contributing significantly to air quality degradation (Masiol and Harrison [2014], Grobler et al. [2019]) and cause for 8.000-12.000 premature deaths annually (Barrett et al. [2010], Yim et al. [2015]).

To increase our understanding of the current and future impact of air traffic on air quality, NO<sub>x</sub> emissions of aviation must be quantified and documented. Measurement campaigns have in general focused on the quantification of NO<sub>x</sub> emissions of the Landing and Take-Off (LTO) cycle, which have been analysed in detail us-

ing ground-based measurements and satellite retrievals (Herndon et al. [2004], Lawal et al. [2022]). Some research efforts have been undertaken to quantify actual emissions of en-route  $\text{NO}_x$  emissions, via in flight campaigns (Schumann et al. [2000]), but no systematic methodology is available to document actual en-route aviation  $\text{NO}_x$  emissions. Annual estimates of  $\text{NO}_x$  en-route emissions are instead generated using theoretical models. These models commonly use a bottom-up approach starting from LTO emission indices based on the International Civil Aviation Organisation (ICAO) engine exhaust emission index inventory. Non-LTO emission indices are extrapolated using the Boeing Fuel Flow Method II developed by Baughcum et al. [1996] such that  $\text{NO}_x$  emissions of the full-flight cycle can be analysed and used to estimate annual global aviation-attributable  $\text{NO}_x$  emissions (Lee et al. [2002], Kim et al. [2007], Wilkerson et al. [2010], Stettler et al. [2011], Quadros et al. [2022b]).

Over the last decades, developments in technology have advanced quantification of global nitrogen oxide pollution. Using satellite observation the entire atmosphere can be sensed such that quantification is no longer confined to local and lower level  $\text{NO}_x$  emissions. The satellite instruments do not measure the combination of nitrogen oxides ( $\text{NO}_x \equiv \text{NO} + \text{NO}_2$ ), instead  $\text{NO}_2$  vertical column densities are retrieved. However, as the emitted  $\text{NO}$  is converted near instantaneously to  $\text{NO}_2$  through a sunlight-induced photochemical process involving ambient ozone (Atkinson [2000], Seinfeld and Pandis [2006]), the measured concentration of  $\text{NO}_2$  can be used as robust measure for  $\text{NO}_x$  concentrations (Koukouli et al. [2021]). In 2017, the European Space Agency (ESA) launched TROPospheric Monitoring Instrument (TROPOMI). This remote sensing instrument uses differential optical absorption spectroscopy to measure nitrogen dioxide concentrations at a high spectral (0.05 nm) and spatial (3.5 km by 5.5 km) resolution and high signal-to-noise ratio (1000) (Veefkind et al. [2012]). The detailed TROPOMI measurements have enabled researchers to detect individual  $\text{NO}_x$  plumes from static and mobile heavy emitters such as power plants (Goldberg et al. [2020]), ships (Georgoulas et al. [2020], Kurchaba et al. [2022]) and mining facilities (Griffin et al. [2019]). Trends in weekly and annual  $\text{NO}_x$  cycles have been investigated (Demetillo et al. [2020], Goldberg et al. [2021]) and overall ground level  $\text{NO}_2$  concentrations have been estimated (Cooper et al. [2020], Chan et al. [2021], Long et al. [2022]). Moreover, detailed validation estimates have been retrieved for upper tro-

pospheric lightning  $\text{NO}_x$  emissions (Bucsela et al. [2021], Allen et al. [2021], Pérez-Invernón et al. [2022]) and for the first time global upper tropospheric  $\text{NO}_2$  samples have been produced (Marais et al. [2021]), greatly advancing knowledge on upper tropospheric nitrogen dioxide behaviour. Due to its temporal overlap with the COVID-19 pandemic, TROPOMI data have been of great value in the assessment of the impact of lockdown restrictions on the total nitrogen dioxide concentrations (Bauwens et al. [2020], Vîrghileanu et al. [2020], Shi and Brasseur [2020], Bassani et al. [2021]) and the anthropogenic contribution therein (Zhang et al. [2021], Koukouli et al. [2021], Shikwambana and Kganyago [2021], Goldberg et al. [2020], Wu et al. [2022]). These achievements suggest that  $\text{NO}_2$  observations by TROPOMI may also prove to be of great value in the systematic documentation of en-route aviation  $\text{NO}_x$  emissions. Studies that have utilised TROPOMI data to quantify aviation-attributable nitrogen oxide emissions have focused on surface level concentrations and have discarded measurements over clouds (Koukouli et al. [2021], Shikwambana and Kganyago [2021] and Lawal et al. [2022]). However, for detection of lightning emissions (Pickering et al. [2016], Zhang et al. [2020], Pérez-Invernón et al. [2022]) and quantification of upper tropospheric mixing ratios (Marais et al. [2021], features of the TROPOMI cloud algorithm have been applied successfully. Scattering and absorption effects within clouds can shield  $\text{NO}_2$  concentrations below clouds from being observed and can enhance the detection of above cloud  $\text{NO}_2$  concentrations. As en-route aviation emissions are likewise expected to be in the upper tropospheric region above clouds, cloudy scenes may also prove useful in the detection of en-route aviation.

A first step towards advances in systematic documentation of actual en-route aviation  $\text{NO}_x$  emissions is to explore the extent to which patterns in nitrogen dioxide measurements of the highest resolution remote sensing instrument currently available (i.e. TROPOMI) can be detected and attributed to en-route aviation. The availability of high resolution measurements, telemetric aircraft observations, and the interesting research window caused by the temporary decline in aviation intensity due to COVID-19 induced travel restrictions, presents a great opportunity for research into relations between remote-sensed nitrogen dioxide levels and emission estimates. In this work, the potential of TROPOMI to detect evidence of aviation-attributable  $\text{NO}_x$  is assessed by comparison of recent and accumulated aviation  $\text{NO}_x$  estimations at an ideal location with actual

retrieved TROPOMI data both over clear sky and cloudy scenes.

## 2. Materials & Methods

### 2.1 Method overview

To analyse whether evidence of en-route aviation activity can be observed by satellite remote sensing and whether cloudy measurements can favour detection chances, the research has been divided into two parts:

1. Firstly, an ideal location for the comparison between en-route aviation  $\text{NO}_x$  emissions and TROPOMI measurements is sought where monthly averaged emissions are compared with satellite retrievals. Aviation intensity, non-aviation  $\text{NO}_x$  sources, and satellite alignment and data quality are considered to maximise the detection chances at the selected location. Emission estimates are computed under unrealistically stable meteorology conditions (i.e. considering no advection or dilution) to favour maximum possible accumulation of emissions. Resulting emission patterns are compared to TROPOMI measurements to determine whether large-scale impact of en-route aircraft emissions on the concentration of nitrogen dioxides can be detected. This strategy is similar to those successfully employed by Beirle et al. [2004] and Richter et al. [2004] to identify maritime  $\text{NO}_x$  emissions over the main shipping corridors from remote sensed  $\text{NO}_2$  data.

2. Secondly, cloudy measurements are analysed separately to determine their influence on measurement precision, and  $\text{NO}_2$  vertical column density retrieval. A search for any evidence of en-route aviation  $\text{NO}_x$  emissions above clouds is conducted. Here, clouds are used as means to separate surface and high altitude  $\text{NO}_x$  concentrations. Monthly measurements are again compared to emission estimates to determine whether large-scale impact of aviation can be observed in TROPOMI measurements. Furthermore, cloudy measurements at recent observations of aviation are analysed for quantitative relations. To reduce influences from advection, which are expected to be significant due to high wind speeds in the upper troposphere, aircraft observations close to the satellite overpass time (max 1000 s) are analysed for differences in downwind and upwind measurements and compared to emission estimates. In the time window between aircraft observation and satellite measurements, plume dispersion and chemistry have not been accounted for and wind is assumed to be constant.

### 2.2 Aircraft observations

To identify aviation activity, satellite observations of Automatic Dependent Surveillance–Broadcast

(ADS-B) data are used. ADS-B is a telemetry technology implemented in modern commercial aircraft. Via ADS-B, aircraft automatically broadcast their identification code and state at frequent time intervals such that air traffic monitoring stations as well as other aircraft can receive the signal. In large parts of the world aircraft flying under instrument flight rules are now required to be equipped with ADS-B as air traffic control is progressively relying upon it, especially in areas with limited radar coverage (FAA [2019], EASA [2020]). The equipment requirement and the growing availability of ADS-B recorders have resulted in useful ADS-B based data collections for aviation research. The ADS-B data collection used in this paper is obtained from global data and analytics company Spire and includes aircraft identification code, longitude, latitude and time observation. The collected aircraft identification codes are linked with Flightradar24 (<https://www.flightradar24.com>) and OpenSky (Strohmeier et al. [2021]) databases to determine the aircraft type code and flight origin and destination.

### 2.3 Aircraft emissions

The Open Aviation Emissions Model (openAVEM) developed by Quadros et al. [2022b] is used to derive the emissions of  $\text{NO}_x$  from en-route aviation activity. This model uses the Boeing Fuel Flow Method 2 (Baughcum et al. [1996]) to derive emission indices from the certification indices to those at altitude whilst taking into account the fuel flow using Base of Aircraft Data (BADA) 3.15 (Mouillet [2017]). Each flight is separately simulated after which the  $\text{NO}_x$  emissions expressed as  $\text{NO}_2$  mass-equivalent are aggregated for the flight set of interest. As large variation in payload was induced by lockdown measures, load factors were taken from International Air Transport Association (IATA) monthly statistics to provide accurate  $\text{NO}_x$  emissions. In the ideal case, flight trajectories are routed such that the fuel burn from origin to destination is minimised. In practice, due to airspace restrictions, weather scenarios, and limited radar coverage over the ocean, minimum distance routes are not always followed. However, to accurately compare flight emissions with satellite measurements the exact location of expected emissions is of key importance. Therefore, the existing openAVEM trajectory algorithm is adapted such that each flight trajectory crosses the median of all flight specific ADS-B (latitude, longitude) observations. In Figure 2.1, a visualisation of two flight trajectories is given. Compared to the initial geodesic trajectories on average an increase of 0.76 % in fuel burn and 0.69 % in  $\text{NO}_x$  is observed.

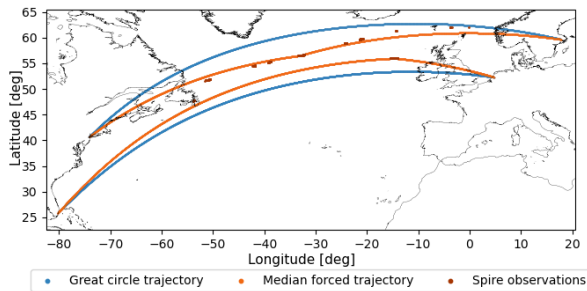


**Figure 2.1:** Differences in original geodesic trajectories and adapted trajectories through observation median.

#### 2.4 Satellite observations

Since April 2018, TROPOMI (Veefkind et al. [2012]) delivers daily measurements of global nitrogen dioxide concentrations. The TROPOMI instrument relies on differential optical absorption spectroscopy (DOAS) in which measured backscattered spectra are fitted against modelled reflectance spectra. The resulting slant column density is compared to a priori estimates to separate tropospheric and stratospheric contributions. Finally, both contributions are converted using air mass factors (AMFs) to obtain the stratospheric and tropospheric vertical column densities. The push-broom staring technique of the sensor allows for a simultaneous observation of 450 measurements along the entire swath width, such that measurements at a spatial resolution of 7.5 km (5.5 km since August 2019) by 3.5 km at nadir can be obtained. The sun-synchronous TROPOMI instrument crosses the equator at 13.30 hr local time. In this research, level-2 tropospheric and stratospheric column data are used (publicly available from <https://s5phub.copernicus.eu/>). TROPOMI level-2 data are extensively validated with data from ground-based spectrometers and its precursor (Ozone Monitoring Instrument, OMI) (Griffin et al. [2019], Lorente et al. [2019], Wang et al. [2019], Ialongo et al. [2020], Zhao et al. [2020], Verhoelst et al. [2021], van Geffen et al. [2022b]). To be able to compare  $\text{NO}_2$  vertical column densities at the same location over multiple days, level-2 data are resampled to common grids at a resolution of  $0.05^\circ$  by  $0.05^\circ$  in monthly analyses.

The absorption spectra measured by TROPOMI which are required to quantify the concentration of nitrogen dioxide in the atmosphere are not only affected by the nitrogen dioxide concentrations in the atmosphere but also by Mie, Raleigh and non-selective scattering. Non-selective scattering and absorption in clouds limits the light that reaches and measures any nitrogen dioxide below the cloud. The retrieval algorithm is adapted consequently. The AMF, needed for

conversion from slant column density to vertical column density, is reduced to zero for the path below the cloud and increased for the above cloud measurements, resulting in averaging kernels enhancing high altitude emissions, as is visualised in Figure 2.2.

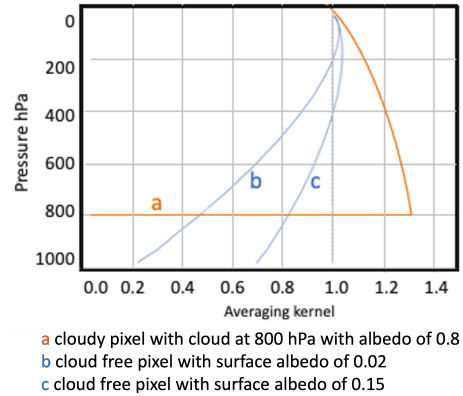


**Figure 2.2:** Example of an averaging kernel for a pixel with an optically thick cloud and averaging kernels for cloud free pixels with varying surface albedo (Eskes and Boersma [2003]).

As aviation en-route emissions are generally located above cloud altitudes, clouds could provide a natural means to separate the lower level emissions from the total columns and increase the detection potential of above cloud aviation emissions. Another potential benefit of using cloudy measurements stems from the better precision of cloudy measurements due to decreased DOAS retrieval uncertainties for higher total radiance signals (van Geffen et al. [2020]).

In this paper the  $\text{NO}_2$ -fitted cloud fraction is adhered to when selecting cloudy measurements for analysis. Cloud fraction is derived by fitting of the continuum reflectance in the nitrogen dioxide retrieval window to a simulated reflectance. In the simulation, the independent pixel approach is applied to model the reflectance as a linear combination of radiative transfer equations for the clear sky part of the pixel and radiative transfer equations for the cloudy part. In this latter, clouds are modelled as single Lambertian reflecting boundaries with an albedo of 0.8. This method is similar to the Fast Retrieval Scheme for Clouds from the Oxygen A band version Sentinel (FRESCO-S) derived cloud fractions but preferred in  $\text{NO}_2$  analysis as the slight misalignment in UV-VIS and NIR products of TROPOMI may yield different cloud fractions (van Geffen et al. [2022a]).

#### 2.5 Meteorological fields

Meteorological fields are obtained from the second Modern-Era Retrospective analysis for Research and Applications (MERRA-2, Gelaro et al. [2017]).

For April 2020 and April 2021, wind fields at 250 hPa have been obtained at native MERRA-2 resolution ( $0.5^\circ$  by  $0.625^\circ$ ) for the hour of maximum plume age until TROPOMI overpass time.

### 3. Results & Discussion

#### 3.1 Comparison at ideal research location

Though having significant impact on climate, air quality and human health, aviation  $\text{NO}_x$  emissions only make a small contribution to the total nitrogen dioxide concentrations. Therefore, selection of a favourable research location may have a large impact on remote sensing detection chances.

##### 3.1.1 Selection of research location

In search of a research location with high potential for detection of en-route aviation attributable  $\text{NO}_x$  by remote sensing several factors have been analysed. First of all, high quality retrievals of TROPOMI must be available. Veefkind et al. [2012] suggest a minimal pixel specific quality assurance value of 0.5 is required for the research location such that only good quality measurements over cloudy and cloud free scenes are included in the data analysis. Computation of the average quality values during the months of analysis indicates this requirement can be fulfilled as long as the research location falls between  $65^\circ$  South and  $65^\circ$  North.

Remote sensing instruments measure total column densities and do not provide information on the vertical distributions such that aviation  $\text{NO}_x$  emissions cannot be easily separated from emissions of other sources. Thence, to maximise detection chances locations are sought that have high aircraft intensity and limited nitrogen dioxide emissions of further anthropogenic and natural sources. Furthermore, the orientation of the main flight routes with respect to satellite overpass direction is preferred in orthogonal direction to allow for as many high quality measurements as possible and low misclassification risk of striping effects. Computation of average flight intensity during the least flown week of the research window and analysis of the rate of emissions of non-aviation sources published in the Community Emissions Data System (CEDS, Smith et al. [2015]), have resulted in the primary selection of a part of the North Atlantic ( $60^\circ$  W -  $10^\circ$  W,  $40^\circ$  N -  $65^\circ$  N), hereafter NA) which stretches from Newfoundland in the West to Ireland in the East and contains the North Atlantic Flight Corridor (NAFC) (Supplemental section 4.1). Maritime traffic between the USA and Europe may also be observed but does in general stay well below the  $45^\circ$  N circle of latitude

such that separation between aviation and maritime traffic emissions may be easily established.

##### 3.1.2 Comparison of satellite measurements with emission estimates

Emissions from en-route aviation over the North Atlantic Flight Corridor during April 2020 and April 2021 are estimated using the openAVEM emission model and converted to petamolecules per squared centimetre to match TROPOMI retrieval measurement units. To maximise detection probability, unrealistically stable meteorology is considered. Furthermore, the maximum plume age of 10 hours reported by Schumann et al. [2000] is adhered to in the derivation of accumulated emissions from undissolved plumes. Using the geographical data and timestamp in the ADS-B message, a selection of flights and their trajectories is generated and fed to openAVEM. The resulting spatial distributions are compared with TROPOMI measurements at common spatial resolution (Supplemental section 4.4).

Analysing the openAVEM estimates in Figure 3.1, a distinct pattern is visible for both April 2020 and April 2021 between the  $47^\circ$  and  $57^\circ$  latitude bands, intensifying near the eastern edge of the North Atlantic Flight Corridor. In the TROPOMI measurements, given in Figure 3.2, no enhancements can be observed over this region. As can be observed in Figure 3.3, increases in  $\text{NO}_2$  column densities that can be expected from en-route aviation emissions do not correspond with increases in the TROPOMI measurements. Monthly averaged winds over the NAFC from MERRA-2 are in eastern direction with negligible meridional wind components, and are not thought to cause latitudinal shifts in  $\text{NO}_2$  vertical column densities. Neither can year-on-year expected increases in  $\text{NO}_x$  solely explain increases in TROPOMI measurements (Figure 3.3).

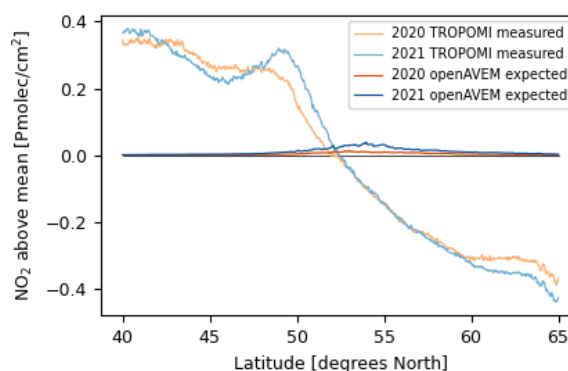


**Figure 3.3:** Zonally averaged measured  $\text{NO}_2$  vertical column densities over the eastern North Atlantic (East of  $35^\circ$  W) and expected peaks from openAVEM as function of latitude.

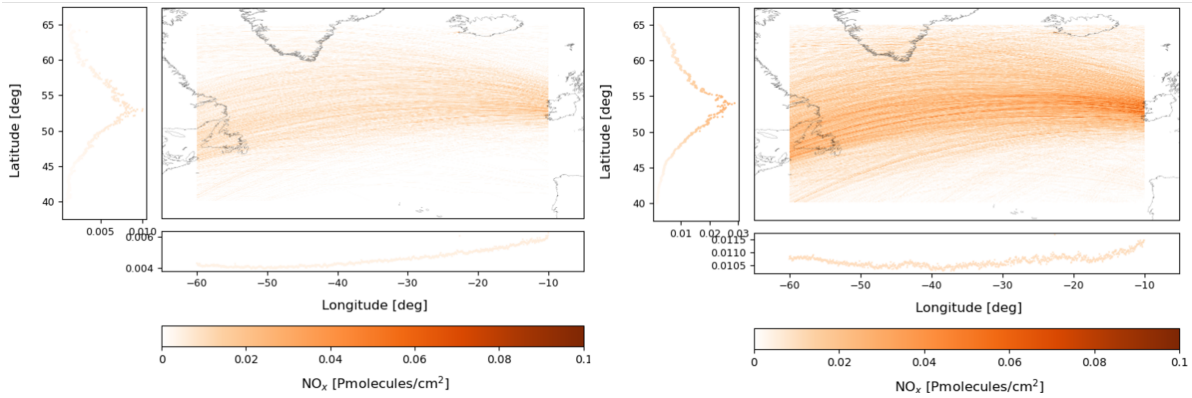


**Figure 3.1:** Average openAVEM expected NO<sub>x</sub> vertical column densities over the North Atlantic during April 2020 (left) and April 2021 (right).

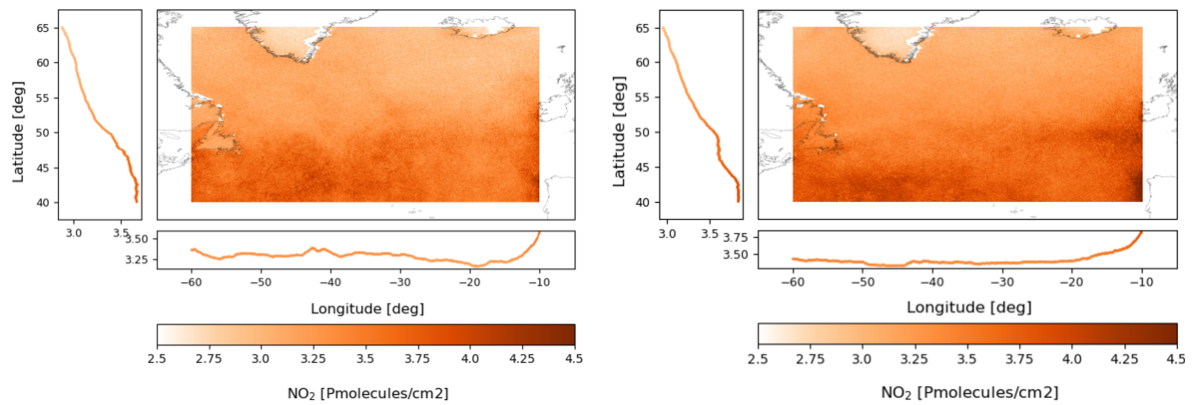


**Figure 3.2:** Average TROPOMI measured NO<sub>2</sub> vertical column densities over the North Atlantic during April 2020 (left) and April 2021 (right).

From analysis of the average TROPOMI precision over the NA, an explanation for the lack of correlation can be found. Even whilst allowing for maximum accumulation of NO<sub>x</sub> from en-route aviation under favourable meteorological circumstances to obtain upper bounds, the measurement precision of TROPOMI is not reached (Figure 3.5), reducing the chances of detection by remote sensing under more realistic conditions including atmospheric dispersion and chemical conversion.

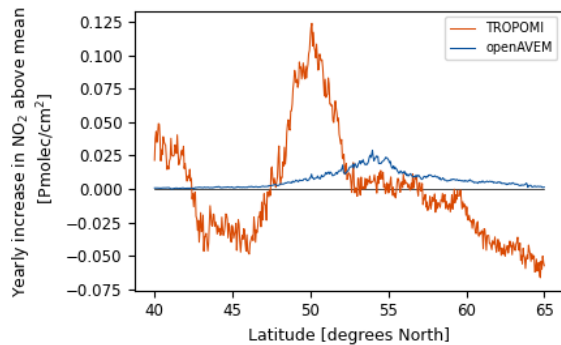


**Figure 3.4:** Zonally averaged year-on-year increases in measured NO<sub>2</sub> vertical column densities over the eastern North Atlantic (East of 35° W) and expected increases in NO<sub>x</sub> from openAVEM as function of latitude.

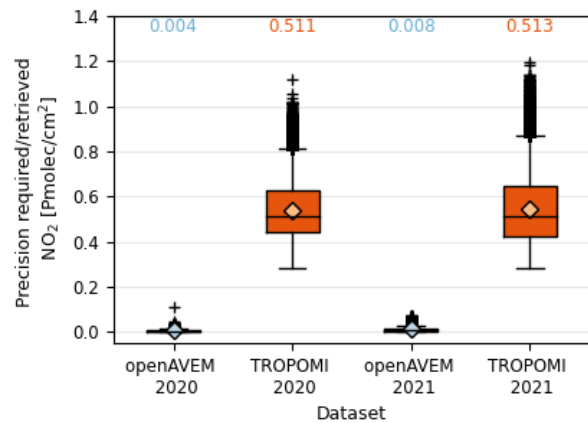


**Figure 3.5:** Monthly averaged expected NO<sub>x</sub> from en-route aviation and TROPOMI measurement precision per 0.05° grid cell. Inset values display medians.

### 3.2 Above cloud evidence search

In efforts to obtain more favourable detection conditions, the TROPOMI data is filtered such that only cloudy scenes are considered. Selecting TROPOMI measurements with high effective radiometric cloud fractions, allows for enhanced sensitivity to above cloud nitrogen dioxide and reduced sensitivity to nitrogen dioxide below clouds.



### 3.2.1 Influences of clouds on TROPOMI measurements

As only limited measurements (1.58 % of measurements over the NA) were available for fully cloudy scenes, TROPOMI measurements with an effective radiometric cloud fraction of 0.75 and larger are considered (Supplemental section 4.2). The measurements over optically thick clouds are in general found to have lower precision uncertainty than those over clear sky scenes, see Figure 3.6. Using the non-parametric Mood's median test, a significant decrease (8.96%) in median precision uncertainty is observed for cloudy measurements over the North Atlantic.

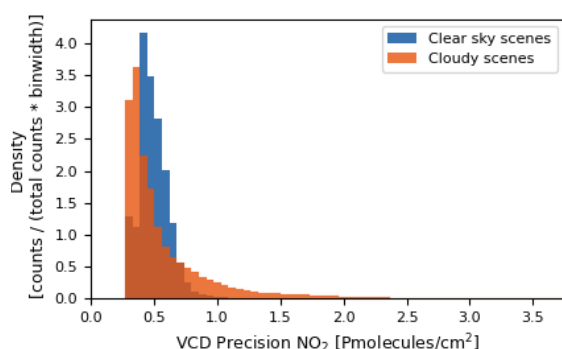


Figure 3.6: Precision of cloudy and clear sky measurements.

Changes in total column density are also observed as shown in Figure 3.7. Cloudy scenes have on average lower total column values, which can be explained by the shielding effect of clouds on lower level emissions.

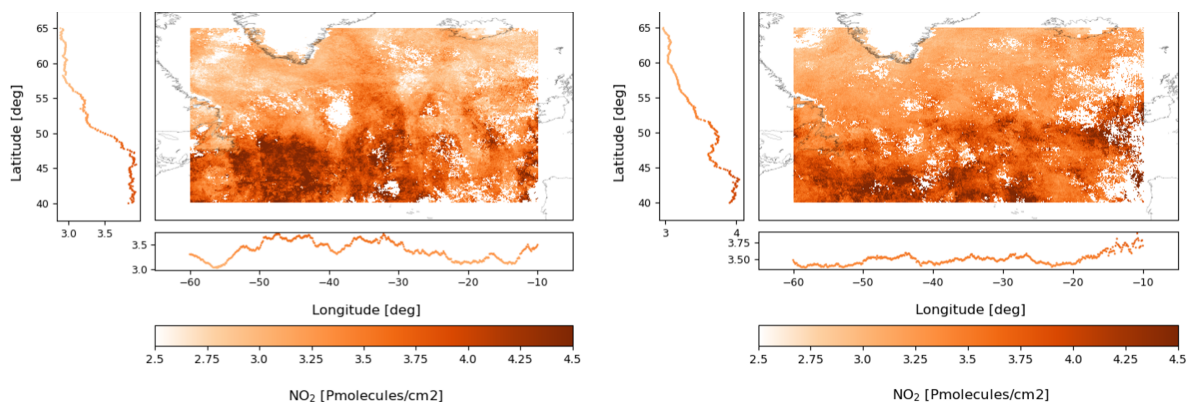


Figure 3.8: Average TROPOMI measured  $\text{NO}_2$  vertical column densities over the North Atlantic over cloudy scenes during April 2020 and April 2021.

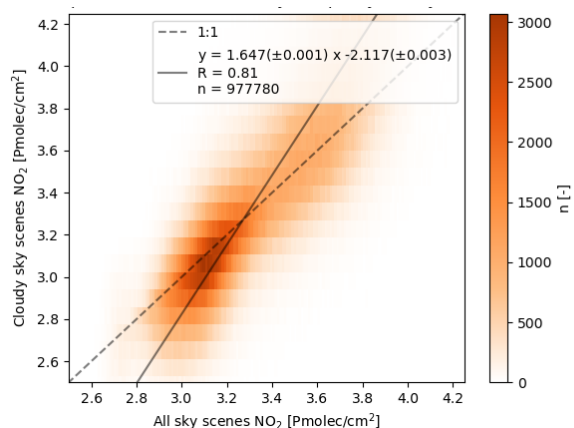
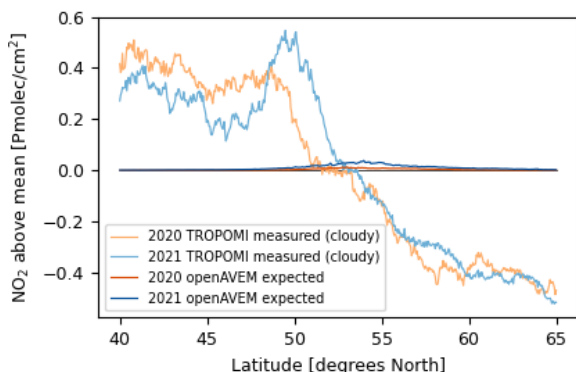


Figure 3.7: Comparison of monthly  $\text{NO}_2$  measurements over all and cloudy only scenes over the North Atlantic.

### 3.2.2 Comparison of average cloudy measurements with emission estimates

To determine whether the selection of just cloudy measurements favours correlation between the spatial distributions, cloudy measurements have again been compared with openAVEM emission estimates. First, a similar approach as for all scene measurements is followed, retrieving monthly averaged spatial distributions in Figure 3.8. Due to the overlap of the research with COVID-19, differences in expected  $\text{NO}_x$  emissions were observed. In 2021, the peak of the pandemic was over and lockdown regulations relaxed such that more flights were identified using ADS-B data (Strohmeier et al. [2021]). However, year-on-year differences observed in TROPOMI measurements over cloudy scenes over the NA fluctuated and could not solely be explained from differences in emission estimates (Figure 3.9, Figure 3.10). Earlier qualitative research by Beirle [2004], using cloudy Global Ozone Monitoring Experiment (GOME) observations and aircraft emission estimates from an emission inventory

(Schaefer et al. [2013]) also did not find indications for aircraft emissions in satellite observations over cloudy scenes over the NA.



**Figure 3.9:** Zonally averaged cloudy measured  $\text{NO}_2$  vertical column densities over the eastern North Atlantic (East of  $35^\circ$  W) and expected peaks from openAVEM as function of latitude.

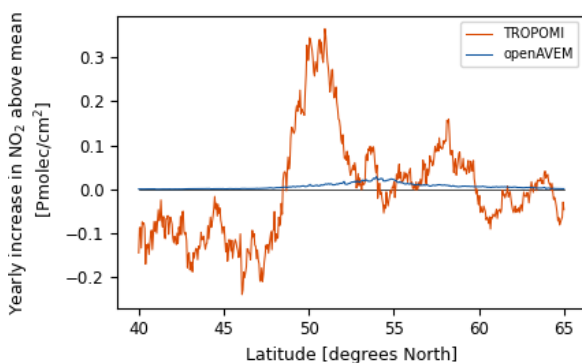


**Figure 3.10:** Zonally averaged year-on-year increases in measured  $\text{NO}_2$  vertical column densities over the cloudy scenes over the eastern North Atlantic (East of  $35^\circ$  W) and expected increases from openAVEM as function of latitude.

### 3.2.3 Comparison of emission estimates from individual aircraft observations with cloudy measurements

The improved median of measurement precision, shown in Figure 3.6, enhanced sensitivity to high altitude nitrogen dioxide concentrations (Marais et al. [2021]), and availability of temporal ADS-B observations encouraged to analyse cloudy measurements for any evidence of recent en-route aviation. Using the ADS-B data points, TROPOMI measurements that could possibly include fresh aircraft plumes containing nitrogen dioxide are identified. Based on the plume dispersion model by Paoli (Tait et al. [2022]), a maximum of 1000 s to overpass time is chosen for fresh plume analysis. Using the closest MERRA-2 retrieved upper tropospheric winds at overpass times, differences in downwind and upwind nitrogen dioxide vertical column measurements within maximum advection radius around the point of aircraft observation are

computed and compared with emission estimates generated using openAVEM to retrieve possible relations between TROPOMI measurements and en-route aviation.

As becomes clear from the distributions in Figure 3.11 and their describing features in Table 3.1, the observed differences in downwind and upwind  $\text{NO}_2$  concentrations contain negative values (i.e. upwind  $\text{NO}_2$  measurements are larger than downwind  $\text{NO}_2$  measurements) whereas for emissions only positive values are expected.

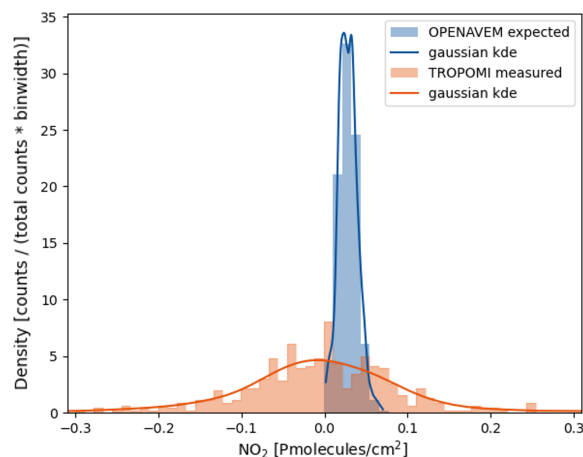


**Figure 3.11:** Comparison of TROPOMI  $\text{NO}_2$  downwind minus upwind measurements at locations of recent aviation activity with openAVEM expectations.

**Table 3.1:**  $\mu$  and  $\sigma$  of distributions given in Figure 3.11

	openAVEM	TROPOMI	
$\mu$	0.028	-0.009	Pmolecules/cm <sup>2</sup>
$\sigma$	0.013	0.109	Pmolecules/cm <sup>2</sup>
n	746	746	nr. of recent aircraft observations for comparison

### 3.3 Factors complicating detection of en-route aviation $\text{NO}_x$ emissions

The inability to detect any evidence of  $\text{NO}_x$  emissions from en-route aviation in this research may have several causes. A first cause, may lie in the low expected emissions. Even whilst considering unrealistically stable weather conditions, in which dilution and advection are neglected for a maximum plume age of 10 hours, the accumulated  $\text{NO}_x$  emissions were found to be lower than the precision of the TROPOMI instrument (Figure 3.5). Analysing areas at times with higher expectations of aviation-attributable emissions, such as airports in pre-COVID-19 years, Lawal et al. [2022], Shikwambana and Kganyago [2021], Kanhiah et al. [2021] could identify relations between aviation and TROPOMI observed nitrogen dioxide



levels. Especially during high engine power operations, such as take-off, nitrogen dioxide emissions indices are higher than those en-route, such that detection probability may be higher at near-airport operations. Furthermore, surface winds are in general lower than those in the upper troposphere reducing influences from advection. However, disentangling flight emissions from ground-based operations such as emissions from non-aircraft at lower altitude levels may prove difficult. The analyses of airports by Shikwambana and Kganyago [2021] and Kanniah et al. [2021] did not separate aerial from ground-based airport operations such that emissions from non-aircraft are still included in the found trends.

Other factors that may complicate the identification of en-route aviation  $\text{NO}_x$  emissions over the NA may be found in the effects of meteorology on nitrogen dioxide. Regional meteorological circumstances can cause larger areas over the NAFC to vary in  $\text{NO}_2$  VCDs. The northern polar vortex, for example, negatively influences the  $\text{NO}_2$  VCDs over the NA during winter and spring due to stratospheric  $\text{NO}_2$  destruction (Beirle [2004]). This results in lower VCD values near the polar region, which was also observed in the monthly average TROPOMI measurements in Figure 3.2 and Figure 3.8. The observed measurements do increase further southwards, where influences from the polar vortex are less and VCDs may be increased by other sources. The climate over the NA typically shows a strong pressure gradient between low polar pressures and high subtropical pressures, denoted as the North Atlantic Oscillation (NAO) (Eckhardt et al. [2003]). When positive NAO indices are encountered, strong westerly winds occur which can induce outflow of polluted air from northern America towards the NA. Such events have been observed by Spichtinger et al. [2001] (Canada to Europe), Stohl et al. [2003] (USA to Europe), Donnelly et al. [2015] (North America to Ireland). From 15-year analysis Deng et al. [2021] concluded that a positive correlation between NAO and North Atlantic VCDs exists. This could also explain the observed higher VCDs in the lower half of the NA in Figure 3.2 and Figure 3.8.

On a local scale further meteorological influences on the concentration levels of  $\text{NO}_2$  may be expected from incoming solar radiation, which controls the kinetics of the photolysis reaction of  $\text{NO}_2$  (Falocchi et al. [2021], Bradshaw et al. [2000]), for which the measurements by Nishanth et al. [2011] during solar eclipse episodes have provided a valuable source of validation. The photo-stationary balance between  $\text{NO}_2$ ,  $\text{NO}$  and  $\text{O}_3$  is further affected by ambient temperature, which con-

trols the reaction rate of the formation of  $\text{NO}_2$  from  $\text{NO}$  and  $\text{O}_3$  (Seinfeld and Pandis [2006]). At higher temperatures, reaction speed increases, which explains the longer lifetimes of  $\text{NO}_2$  in the upper troposphere, together with lower  $\text{O}_3$  concentrations due to the lower air density, found by Lamsal et al. [2010]. Further influences may stem from factors that affect the formation of nitric acid ( $\text{HNO}_3$ ) and dinitrogenpentoxide ( $\text{N}_2\text{O}_5$ ), the major sinks of  $\text{NO}_2$ . High relative humidity, for example, enhances the formation of nitrates from nitrogen oxides which may then react to  $\text{HNO}_3$  and  $\text{N}_2\text{O}_5$  (Mentel et al. [1996], Qin et al. [2017]). Finally, the stability of the troposphere is also of importance. High pressures lead to low atmospheric circulation such that nitrogen dioxide concentrations can build up, whereas high planetary boundary layers and high wind speeds (common in the upper troposphere over the NA) may lead to quicker dispersion and dilution of emitted species (Zhang et al. [2021]). These meteorological factors may cause changes in nitrogen dioxide abundance that mask trends induced by changes in emissions (Anh et al. [1997], Grange et al. [2018]). Barré et al. [2021] show that differences in TROPOMI observed  $\text{NO}_2$  concentration levels between COVID and pre-COVID-19 years could be explained by changes in meteorological conditions. In Supplemental section 4.6, a first estimate is generated for the extent of meteorological attributable nitrogen dioxide variations during April 2020 and April 2021 over the NA.

In the generation of TROPOMI  $\text{NO}_2$  VCDs, measured backscattered spectra are fitted against reflectance spectra, which are modelled using, amongst others, weather and assumptions on the vertical density profile of  $\text{NO}_2$  from the chemical transport model (CTM) at  $1^\circ$  by  $1^\circ$  (Williams et al. [2017]) to compute AMFs. In research into LTO operations near Atlanta Airport, Lawal et al. [2022] found that replacing the given a priori profiles by a high resolution (4 km by 4 km) regional chemical transport model reduced the uncertainty in the AMFs, increasing potential for use of satellite observations to evaluate high  $\text{NO}_x$ -emitters such as airports. Similarly, research by Pickering et al. [2016], Bucsela et al. [2019], Allen et al. [2019] and Pérez-Invernón et al. [2022] showed that detection and quantification of lightning flash emissions was possible by creating specific AMFs for (TROP)OMI pixels over lightning. Marais et al. [2021] found that particularly in the upper troposphere, errors in AMF stemming from a priori assumptions on the vertical distribution and coarser CTM may impact the satellite retrievals above clouds. To reduce influences hereof, specific AMFs for cloudy scenes

were generated that only account for viewing geometry in the upper troposphere. Georgoulas et al. [2020] also computed geometric AMFs in their search for shipping plumes to derive more distinct plume structures and to confirm found structures are not artifacts of the retrieval algorithm. In Supplemental section 4.3, an analysis of  $AMF_{geo}$ -retrieved  $NO_2$  VCDs over the NA is provided, which did not yield improved detectability of en-route aviation. Creating more specific AMFs for en-route aviation using measurements of vertical  $NO_2$  profiles in aircraft corridors could potentially increase the detection potential of upper tropospheric en-route aviation  $NO_x$  emissions. However, AMFs for cloudy scenes are already sensitive to above cloud  $NO_2$  concentrations (Figure 4.9), whereas lower level altitude emissions of the LTO operations as those in Lawal et al. [2022] are less enhanced in the given AMFs and emissions of lightning as those in Pickering et al. [2016] create local but high  $NO_x$  emissions, which change vertical profiles and AMFs significantly.

Finally, it must be stipulated that the research presented here relied on ADS-B and TROPOMI data from just two months with limited aviation intensity. Thence, limited data was available, especially when also introducing a cloud factor condition, such that more extensive research may yield more promising and robust results.

#### 4. Concluding Remarks

En-route aviation  $NO_x$  emissions contribute to air quality degradation, affecting human and ecological health. To increase understanding of current and future effects of en-route aviation and to be able to form adequate mitigation measures, actual  $NO_x$  emissions must be quantified and documented. Promising results from previous research projects have shown the capability of remote sensing instrument TROPOMI to detect individual plumes from static and mobile heavy emitters and upper tropospheric weather phenomena. This, together with improved aircraft localisation from ADS-B data, showed potential for the detection and documentation of actual en-route aviation  $NO_x$  emissions by remote sensing. In this research, a first assessment of the potential of TROPOMI to detect evidence of monthly and near-overpass emissions over a favourable measurement location is performed. Actual aircraft observations have been used to generate emission estimates which could be compared with satellite observations. Analysis of monthly estimates created under unrealistically stable atmospheric

conditions (i.e. considering no advection or dilution) to favour maximum emission accumulation showed that upper bounds were lower than detection limits associated with TROPOMI  $NO_2$  VCDs and did not show up as enhanced spatial distributions in satellite observations. Creating more favourable circumstances for analysis by considering cloudy scenes only, which were found to in general have better precision and higher sensitivity to high altitude emissions, likewise yielded uncorrelated results. Neither did fresh plume analysis retrieve any evidence of en-route aviation. Apart from lack of emissions during the COVID-affected research window, difficulties for remote sensing of en-route aviation  $NO_x$  emissions can be linked to their location in the atmosphere. At altitudes of aviation influences from meteorology and long range transport may complicate detection of aviation emissions. Satellite retrievals are further limited in precision due to uncertainties in slant column retrieval and conversion to vertical densities.

From the absence of any evidence of relations between aviation emission estimates and TROPOMI  $NO_2$  VCD retrievals can be concluded that current TROPOMI retrievals do not suffice for detection of en-route aviation emissions in the North Atlantic Flight Corridor during April 2020 and April 2021. As the data set comprised of April 2020 and April 2021 is limited both in size and aviation intensity, future research may seek to increase detection potential by expanding the data set with years that do include higher aviation intensity (e.g. pre-COVID). To reach the precision limits associated with TROPOMI  $NO_2$  VCD retrievals, local emissions must accumulate to over  $0.3 \text{ Pmolecules/cm}^2$ . The emissions over the North Atlantic Flight Corridor that could be expected from openAVEM showed a large variety in flight trajectories such that accumulation of emissions was limited and future detection potential may lie in the analysis of more congested flight routes, such as the airways leading into terminal manoeuvring areas. Furthermore, the pure filtering of TROPOMI data at a favourable research location may be extended with alterations of air mass factors for aviation pixels and corrections for influences from meteorology. Considering current satellite capability and circumstances, detection and documentation of en-route aviation  $NO_x$  emissions by means of the highest resolution remote sensing satellite to date remains a continuous challenge in the near future.

## Conclusion and recommendations

Excessive emissions of nitrogen oxides by en-route aviation alter the Earth's atmospheric composition leading to a degradation of air quality. The effects are not confined to the region of emission but can via long-range transport affect human and ecological health in vast regions of the world, thought to cause over 8000 premature deaths annually. Thusfar, efforts to quantify and document en-route aviation emission were in general model-based as limited means were available to measure upper tropospheric nitrogen oxides.

In an attempt to enable future quantification and documentation of actual en-route aviation emissions, in this research, satellite retrievals of the current most sophisticated remote sensing instrument TROPOMI are assessed for their use in detection of en-route aviation  $\text{NO}_x$ . This was done by comparison of monthly average and near overpass individual emission estimates with satellite retrievals over a favourable location for the months of April 2020 and April 2021. Emission estimates were generated using the openAVEM model and observed flight tracks under unrealistically stable assumed weather conditions to allow for maximum accumulation. Satellite retrievals were filtered for data quality and cloud fraction to obtain retrievals with high detection potential.

From analysis of TROPOMI retrieval quality, aviation intensity, non-aviation anthropogenic emissions and trajectory orientation it was found that the North Atlantic Flight Corridor within the North Atlantic Ocean has most detection potential, as aviation forms the main anthropogenic emission source, good quality satellite data can be retrieved and orientation of the major flight corridor is orthogonal to satellite ground track such that multiple satellite overpasses can be acquired per day and striping effects are limited. It was found that, if available, cloudy skies may increase further research potential as they are found to have lower precision uncertainties than clear sky measurements and can shield surface level concentrations via non-selective scattering and absorption.

Comparison of the monthly average estimated en-route aviation  $\text{NO}_x$  emissions with TROPOMI retrievals over all sky scenes and cloudy skies only did not yield any indication of possible relations. Expected increases in zonal averages did not correspond with retrievals. Analysis of expected emissions from aircraft observed just before ( $\leq 1000$ s) satellite overpasses over cloudy skies did not yield corresponding distributions either.

The inability to detect any evidence of en-route aviation attributable  $\text{NO}_x$  may be caused by several factors. First of all, average estimates of aviation  $\text{NO}_x$  under favourable circumstances did not accumulate to precision limits of TROPOMI for the months of analysis. Furthermore, contributions from large-scale weather phenomena such as the polar vortex, local atmospheric composition and meteorology, and long range-transport from continental  $\text{NO}_x$  sources may mask the limited emissions of en-route aviation. Lastly, uncertainties in sensing capabilities and artefacts from coarser a priori profiles may complicate detection of the locally emitted en-route aviation  $\text{NO}_x$ .

Therefore, it is concluded that nearly 20 years after Beirle [2004] first researched the possibility of satellite detection of en-route aviation, this still remains a challenging task, not achievable by pure filtering of satellite retrievals over favourable locations during the months of April 2020 and April 2021.

---

## Recommendations

Although the observed gap between satellite precision and maximum accumulation of emissions is large and the absence of correlations do not sketch a fruitful basis for future research, some recommendations are given for future research that may result in higher detection potential.

First of all, researchers may strive to expand the research window such that periods with higher aviation intensity may be included and the gap between satellite precision and maximum accumulation of emissions can be closed. Care must be taken when expanding to pre-COVID years as satellite retrievals before the 6<sup>th</sup> of August 2019 have coarser resolution and updates in the retrieval algorithm have since occurred.

This research suggests that meteorology can have a significant impact on the retrieved NO<sub>2</sub> VCDs over the North Atlantic. Therefore, future research efforts may strive to include meteorology decoupling measures in the comparison, for example, by means of a chemical transport model.

Observed en-route aviation NO<sub>x</sub> emissions over the NAFC during April 2020 and April 2021 were limited in magnitude and emitted very locally. However, the air mass factors needed for the conversion of slant to vertical column densities are partly based on meteorology and a priori profiles derived using coarser (1° by 1°) models. Promising results have been achieved in the detection of lightning and near surface aviation emissions when altering AMFs using more specific vertical profiles, such that future research ventures may explore whether detection likelihood can increase when adjusting AMFs for en-route aviation.

Lastly, the accumulation of en-route aviation-attributable NO<sub>x</sub> which may be detected in satellite observations in this research heavily depends on the assumptions on plume age. More research into micro- and large-scale plume chemistry would benefit the accuracy of the retrieved result here and could open opportunities for new research ventures with increased detection potential.

# Supplements

## 4.1. Location

Global aviation emissions form an increasingly significant hazard to air quality levels. Over the past 25 years aviation fuel burn and thus carbon dioxide emissions have annually increased by 2.6% on average (International Energy Agency 2017). Due to the trend in engine designs to operate at higher gas temperatures to strive for more efficient fuel combustion,  $\text{NO}_x$  emissions are increasing at an even higher rate (Grobler et al. [2019]). Though having significant impact on climate, air quality and human health, aviation  $\text{NO}_x$  emissions only make a small contribution to the total nitrogen dioxide concentrations. Therefore, selection of a favourable research location may have a big impact on remote sensing detection chances. Remote sensing instruments measure total column densities and do not provide information on the vertical distributions such that aviation  $\text{NO}_x$  emissions cannot be easily separated from emissions of other sources. Thence, to maximise detection chances locations are sought that have high aircraft intensity and limited nitrogen dioxide emissions of further anthropogenic and natural sources. Furthermore, the orientation of the main flight routes with respect to satellite overpass direction and coverage capability are considered to allow for as many high quality measurements as possible.

A primary requirement for the research location is the availability of high quality satellite data. Eskes et al. [2019] suggest a minimal quality assurance value of 0.5 must be available for the research location such that only good quality measurements over cloudy and cloud free scenes are included in the data analysis. From the computed average in Figure 4.1, one can deduce that as long as the research location falls between 65 degrees South and 65 degrees North, high quality data should be available.

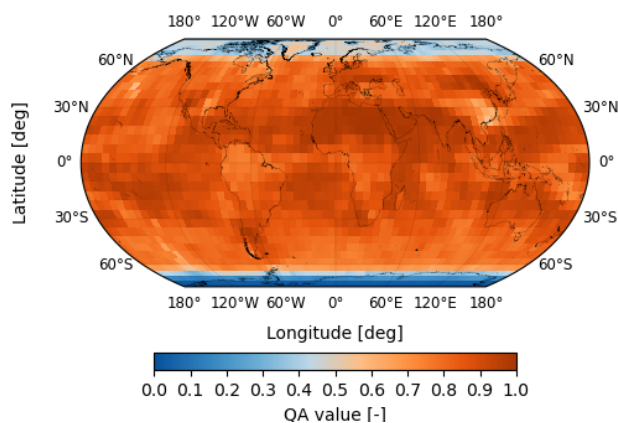


**Figure 4.1:** Average quality assurance value of TROPOMI measurements.

Apart from high quality TROPOMI measurements, it is of key importance for the comparison of emission estimates with measured nitrogen dioxide levels that aircraft are observed frequently over the research location. Areas with good quality measurements that do contain multiple aviation observations even during the least flown week can be found over the USA, Europe and South East Asia, as

well as the flight corridors over the North Atlantic and North Pacific Ocean as can be deduced from Figure 4.2 and Figure 4.3.

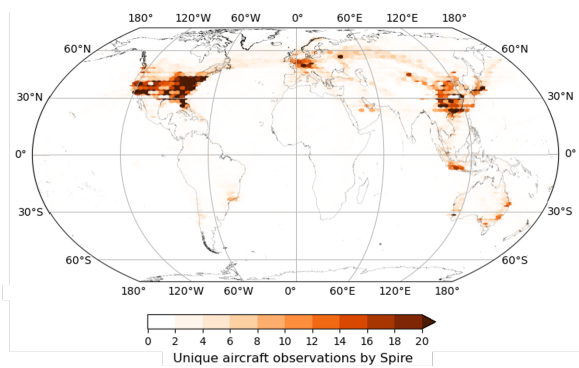


**Figure 4.2:** Aviation intensity during the least flown week.

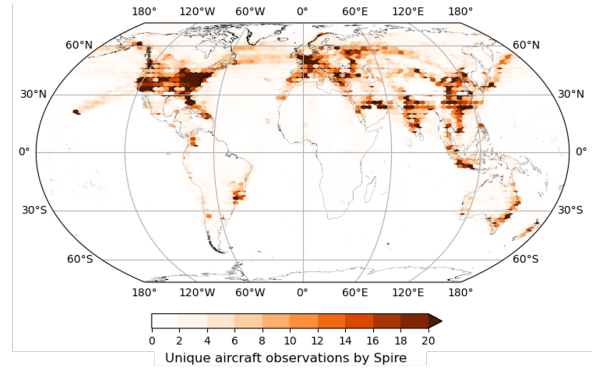


**Figure 4.3:** Aviation intensity during the most flown week.

To identify the regions with high aviation intensity where aviation may be the major anthropogenic source the rate of emissions of non-aviation sources for the most recent month of April published in the community CEDS inventory (Smith et al. [2015]), is analysed. The high rates over the Eastern part of the United States, Europe and South East Asia, as visible in Figure 4.4, suggest these areas may have lower detection potential and that in flight corridors over the oceans aviation may be the major anthropogenic source.

Finally, the orientation with respect to TROPOMI scan lines is considered. Locations with major longitudinal flight trajectories are preferred over those with latitudinal direction. Longitudinal oriented locations will be covered by multiple TROPOMI overpasses such that chances of obtaining high quality satellite measurements will be higher. Furthermore, longitudinal flight trajectories have the advantage that stripes resulting from TROPOMI pixel dependent offsets, such as those shown in Figure 4.5, will have an orthogonal direction and are less likely to be confused with.

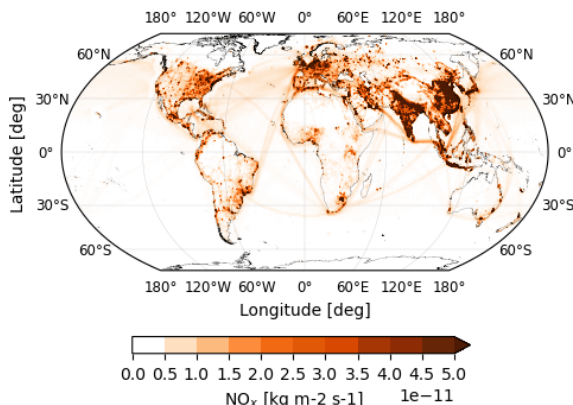


**Figure 4.4:** Average rate of non-aviation anthropogenic emissions during April 2019.

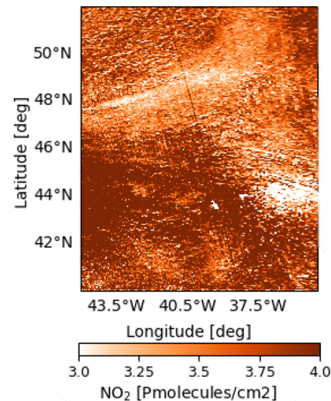


**Figure 4.5:** Example of a stripe (from 38° W, 40° N towards the upper left (41° W, 52° N) created by pixel dependent offsets that may be confused with en-route aircraft emissions

The criteria for high aviation intensity, low non-aviation emissions and good TROPOMI compatibility have resulted in the primary selection of a part of the North Atlantic (60° W - 10° W, 40° N - 65° N) which stretches from Newfoundland in the West to Ireland in the East and contains the North Atlantic Flight Corridor (NAFC). Maritime traffic between the USA and Europe may also be observed but does in general stay well below the 45° N circle of latitude such that separation between aviation and maritime traffic emissions may be easily established.

## 4.2. Cloud fraction

In the performed research a radiometric cloud fraction of at least 0.75 is adhered to for cloudy measurements. If one desires to completely shield lower nitrogen dioxide concentrations measurements with a radiometric cloud fraction of 1.0 should be considered only. A primary reason for relaxing the cloud fraction constraint to 0.75 is given in the number of days and individual measurements available for analysis, increasing from 1.58 % to 22.1 % of the total number of measurements (Figure 4.6). Doing so increases the monthly mean observed values on average by 11.8 %, see Figure 4.7, which can be explained by the shielding effect of the increased cloud cover. When using a cloud factor of 1, too little measurements are found for spatial analysis (Copernicus [2020], Figure 4.8).

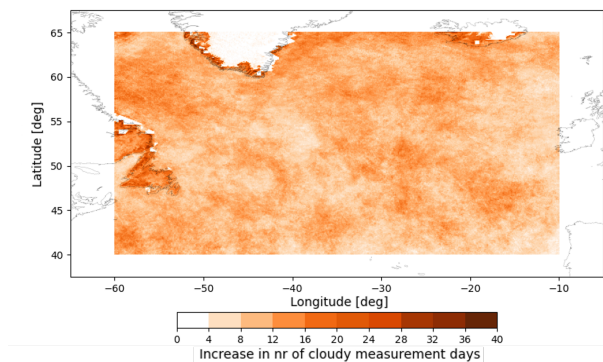


**Figure 4.6:** Increase in available days for analysis when relaxing the cloud fraction condition from 1.0 to  $\geq 0.75$

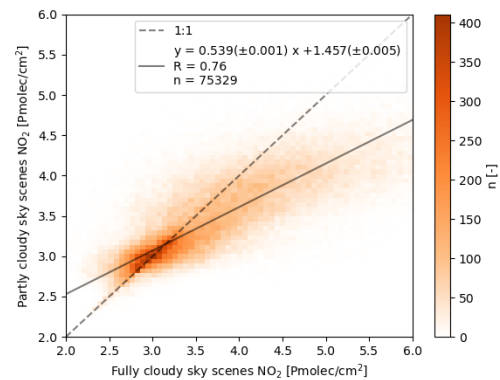


**Figure 4.7:** Comparison of  $\text{NO}_2$  VCD measurements over fully ( $\text{CF} = 1$ ) and partly ( $\text{CF} \geq 0.75$ ) cloudy scenes

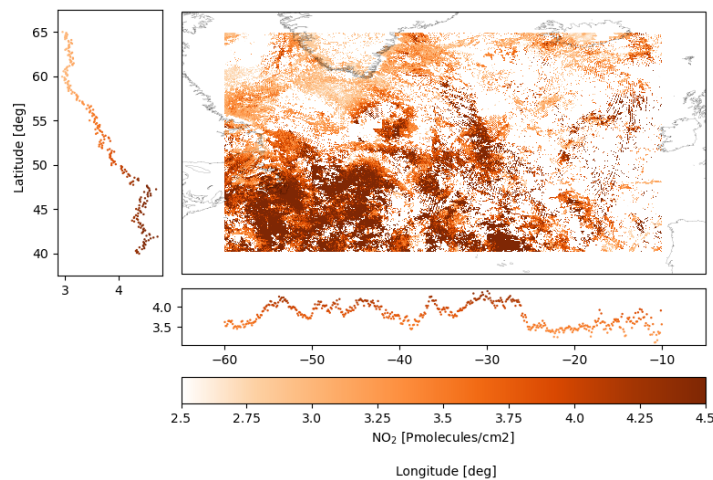


**Figure 4.8:** Average TROPOMI retrievals when considering  $\text{CF}=1$

## 4.3. Air Mass Factor

The analysed vertical column densities of TROPOMI are computed with detailed AMFs which affect the specific individual vertical column values and monthly averaged nitrogen dioxide concentrations retrieved over the NAFC. In the TROPOMI retrieval of upper tropospheric  $\text{NO}_2$  vertical column densities the largest error source is found in the conversion of slant to vertical column densities. Travis et al. [2016], Marais et al. [2021], Silvern et al. [2019], evaluated chemical transport models and satellite measurements with in-situ tropospheric measurements finding discrepancies in the upper troposphere. Silvern et al. [2019], Stavrakou et al. [2013], Travis et al. [2016], Marais et al. [2021]) suggest that these errors may stem from uncertainties in the a priori modelled vertical distribution in the upper troposphere, uncertainties in the kinetics of the photostationary balance between  $\text{NO}_2$ ,  $\text{NO}$  and  $\text{O}_3$ , and errors from



estimates at coarser resolution. In Figure 3.6, already some insight is gained into the magnitude of vertical column density error when adhering to the air mass factors as provided in the TROPOMI retrieval algorithm. To gain some more insight into the magnitude of the possible uncertainty and potentially increase detection probability, Marais et al. [2021] suggest an averaging kernel can be composed that purely accounts for the geometric difference in slant path and vertical path of the upper tropospheric (above cloud) contribution but does include averaging kernels for the stratospheric component.

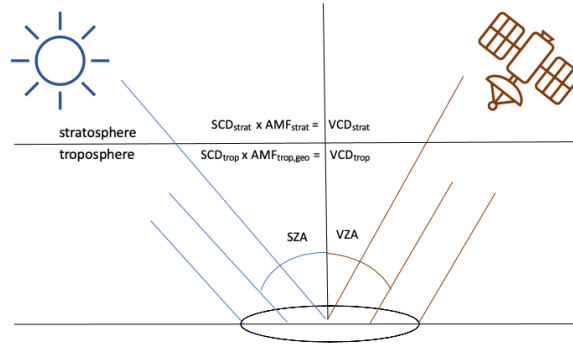


**Figure 4.9:** Visualisation of separation of geometric and detailed AMFs per atmospheric section

Following Marais et al. [2021], the total above cloud vertical column densities are then computed as in Equation 4.1. In Figure 4.9, a visualisation of the vertical column computation of the stratospheric and tropospheric contribution is given as well as a visualisation of the solar zenith angle (SZA) and viewing zenith angle (VZA).

$$VCD_{tot} = VCD_{trop} + VCD_{strat} \quad (4.1)$$

$$VCD_{tot} = \frac{SCD_{trop}}{\sec(SZA) + \sec(VZA)} + VCD_{strat}$$

$$VCD_{tot} = \frac{SCD_{tot} - VCD_{strat} \cdot AMF_{strat}}{\sec(SZA) + \sec(VZA)} + VCD_{strat}$$

Computing the absolute and relative difference over the North Atlantic, it is found that the TROPOMI AMF gains higher values in general (Figure 4.10, Figure 4.11), however, over the flight corridor differences remain well below 10%, similar to the differences observed by Marais et al. [2021] and Choi et al. [2014] using (TROP)OMI measurements over cloudy scenes over the entire globe.

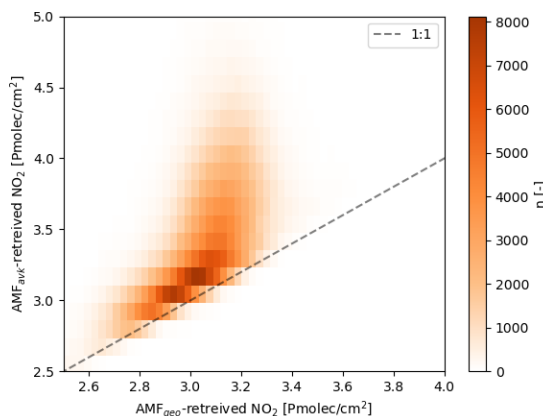


**Figure 4.10:** Absolute difference in average geometric and TROPOMI AMF computed VCDs over the NAFC

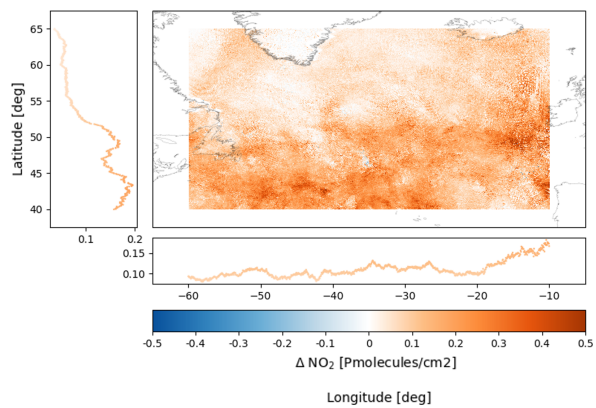


**Figure 4.11:** Difference in average geometric and TROPOMI AMF computed VCDs over the NAFC



The limited changes in TROPOMI have not resulted in improved detectability in monthly trends (Figure 4.12). Expanding the geometric computation of the averaging kernel to the stratospheric part does not yield significant changes relative to the tropospheric part only as in Figure 4.13. This can be explained by the limited contribution of the stratosphere in general and the rather stable meteorological conditions.

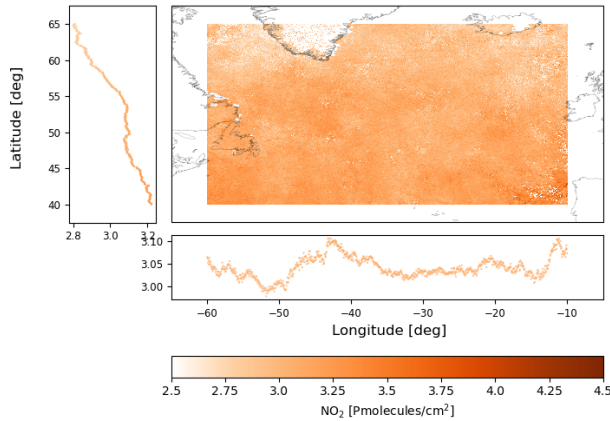


**Figure 4.12:** Average  $AMF_{geo,trop}$ -retrieved TROPOMI  $NO_2$  VCDs over the NAFC

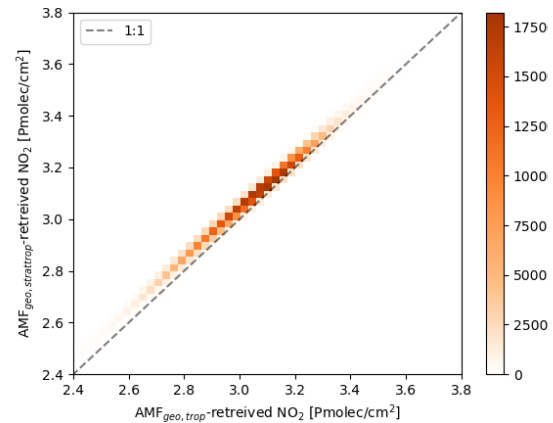


**Figure 4.13:** Difference in  $NO_2$  VCDs when applying a geometric kernel to both the stratospheric and tropospheric contribution and when applying it solely to the tropospheric contribution

Recent research (Pickering et al. [2016], Allen et al. [2019], Bucselo et al. [2019]) into lightning emissions have been able to determine flash density using specific air mass factors for lightning. These are computed by dividing the lightning  $NO_2$  slant column densities modelled using radiative transfer equations and a priori vertical profiles by a model derived specific for vertical column density for lightning. This could have potential for aviation  $NO_x$  emissions as well. However, lightning  $NO_x$  emissions are much more intense than emissions resulting from en-route aviation such that they would alter vertical profiles significantly whereas from aviation little changes in profiles may be expected. Therefore, this approach is not yet investigated in this research.

## 4.4. Resolution

As TROPOMI follows a sun-synchronous trajectory it has the capability to retrieve measurements over the entire Earth each day. This, however, also means that each day the orbits passing over the North Atlantic have a slightly different orientation. Therefore, to compare measurements over multiple days, a common grid must be created with a certain fixed resolution. In this research, when needed a standard resolution of 0.05 by 0.05 degrees is adhered to, as this is close to the average TROPOMI pixel size over the NAFC and results in reasonable computation times. Satellite retrievals are first averaged daily over the chosen resolution before monthly computations. The resolution of the analysis affects the emission estimates from openAVEM. A coarser spatial resolution results in lower emissions per grid cell as emissions are spread over the full area of the grid even when observed only locally. Similarly, peaks of high  $NO_2$  concentration levels are less defined in TROPOMI retrievals when resorting to coarser resolutions. Changing the resolution of  $0.05^\circ$  by a factor 2 to  $0.1^\circ$  reduces the average emission estimates by 44 %; when coarsening the resolution with a factor 10 to  $0.5^\circ$ , a reduction of 76 % can be expected. Coarsening the resolution increases the discrepancy in retrieved and required accuracy, such that detection potential reduces.

Individual orbits have also been analysed at measurement resolution for traces of aircraft evidence. Per orbit, plume-like structures are identified. To confirm these structures are not artefacts of the retrieval algorithm, the scene is also analysed using a geometric AMF. In few cases, plume-like structures were found near aviation observations. In Figure 4.14 an example is given for orbit 18178 in which such plume-like structures near recent telemetric observed aircraft could be identified and persisted in

AMF<sub>geo</sub> retrieved measurements (Figure 4.15).

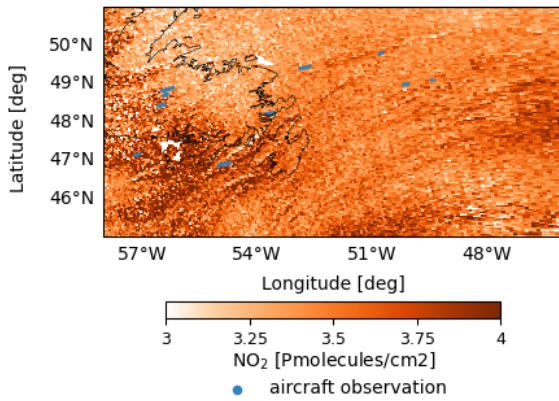


**Figure 4.14:** A plume-like structures in the retrieved TROPOMI NO<sub>2</sub> VCDs can for example be observed between the aircraft observations at (53° W, 49.5° N) and (50.5° W, 49.75° N)

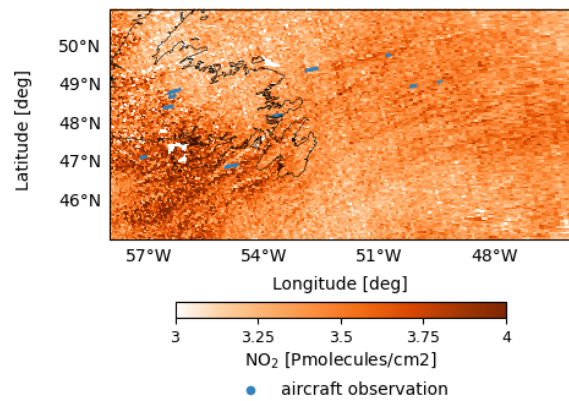


**Figure 4.15:** Persisting plume-like structures in AMF<sub>geo</sub>-retrieved NO<sub>2</sub> VCDs near aircraft observations over the same scene

Although the plume-like structures are in close proximity of aircraft observations, computation of the cloud factor in Figure 4.16 shows that a likely cause for these structures can be found in differences in cloudiness. The shape of the observed plume-like structures corresponds with the narrow clear sky retrieved pixels between cloudy scenes. Therefore, the enhanced NO<sub>2</sub> concentrations may have resulted from shielding of NO<sub>2</sub> at adjoining cloudy scenes instead of aviation emissions. This is supported by the observation of plume-like structures in absence of aviation that could also be linked to differences in cloudiness. Reducing the masking effects of cloudiness by analysing only cloudy scenes or only clear sky scenes unfortunately did not yield further insights. In no cases could persisting plume-like structures be found that could solely be linked to aviation. A cause for the inability to find plume-like structures that are caused by en-route aviation may be because of the low emission strength of aviation emissions, which was found to be below precision thresholds associated with the TROPOMI instrument, dilution of plumes and influences from local-scale meteorology.

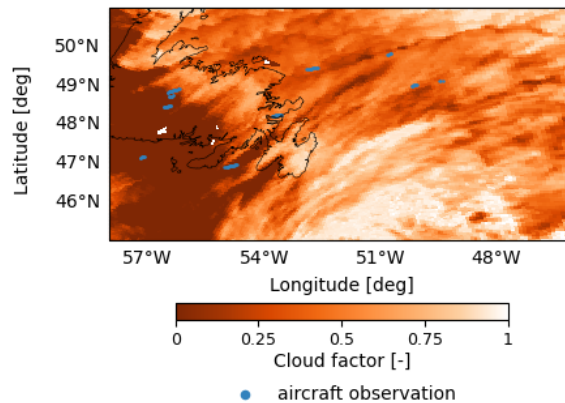


**Figure 4.16:** Cloudiness over the scene in which the plume-like structures are observed

## 4.5. NO<sub>x</sub> plume age and mixing ratios

In the upper troposphere lifetimes of NO<sub>x</sub> emissions are larger than those emitted at surface level due to lower temperatures and O<sub>3</sub> concentrations. Therefore, aircraft emission plumes persist and can accumulate. In the research, a maximum was sought for the accumulation of NO<sub>x</sub> emissions such that maximum reported plume age was used in emission calculations. Although the resulting correlation does not improve when reducing the plume age window, an expectation of the reduction in accumu-

lated emissions is given in Figure 4.17 considering the minimum reported plume age (Schumann et al. [2000]) of 3 hours. In general, a 40 % decrease in emissions is observed when reducing the plume age as shown in Figure 4.18.

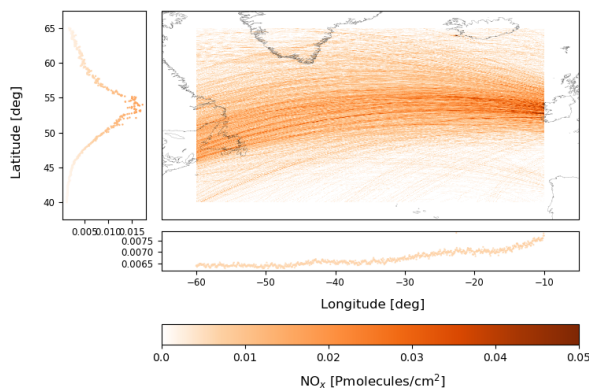


**Figure 4.17:** Average April 2021 emission estimates from openAVEM when considering a 3 hour plume age

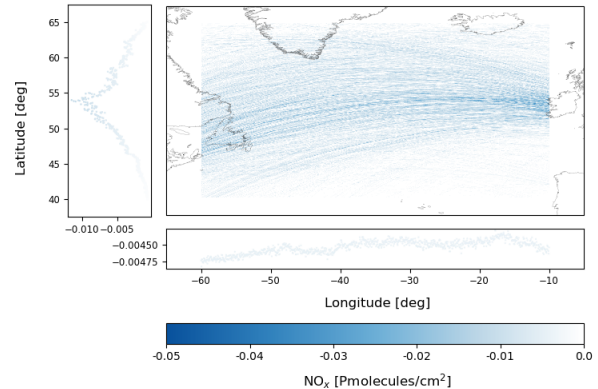


**Figure 4.18:** Absolute difference in expected emissions when decreasing plume age from 10 to 3 hours

The ratio of  $\text{NO}_2/\text{NO}$  of aviation emissions can vary significantly throughout the flight cycle and per engine. Research by Wormhoudt et al. [2007] showed that at high power settings only 7 % of  $\text{NO}_x$  may be in the form of  $\text{NO}_2$ , whereas at low power settings 80 % of  $\text{NO}_x$  may be in the form of  $\text{NO}_2$ . Furthermore, once emitted the conversion of  $\text{NO}_2$  to  $\text{NO}$  and vice versa depends on local meteorology and atmospheric composition. In general,  $\text{NO}_2$  is deemed a good proxy for  $\text{NO}_x$  emissions (Koukoulis et al. [2021]). However, actual values of  $\text{NO}_2$  may be much lower as Ziereis et al. [2000] derived by means of in-situ measurements a ratio of 0.42 for  $\text{NO}_2/\text{NO}_x$  in the upper tropospheric flight corridors. More research into micro-scale  $\text{NO}_x$  chemistry may be required to consolidate actual ratios of  $\text{NO}_2/\text{NO}$  at engine exits and during plume dispersion. Although, the correlation between satellite retrievals and emission estimates will not improve by reducing the  $\text{NO}_2$  ratio an indication of monthly average emission estimates is given in Figure 4.19 for the observed 0.42  $\text{NO}_2/\text{NO}_x$ -ratio which may help identify future remote sensing requirements for en-route aviation emission detection.

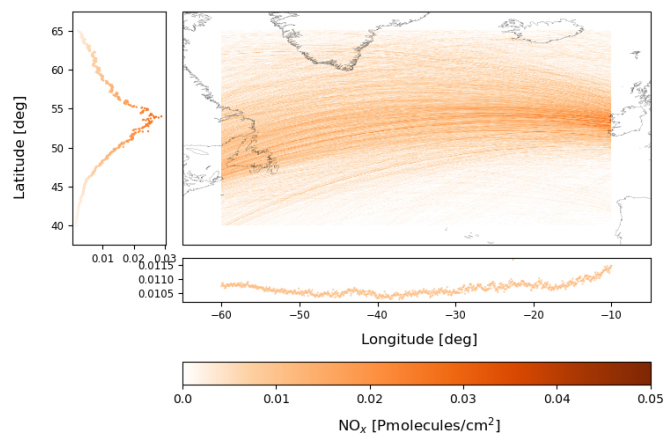


**Figure 4.19:** Emission estimates when considering the reported  $\text{NO}_2/\text{NO}_x$ -ratio of 0.42

## 4.6. Meteorology

To quantify to what extent variation in the TROPOMI measured nitrogen dioxide concentration levels could be attributed to meteorology, a random forest model was built and trained using three years

of tropospheric TROPOMI and MERRA-2 meteorology data over the selected areas of the North Atlantic. The function `RandomForestRegressor` of the python package `scikit-learn` for high computing performance (Pedregosa et al. [2011]) was used to build a regression model with 300 trees based on the models used by Grange et al. [2018], Vu et al. [2019] and Wu et al. [2022], which were used to determine the effects of emission stringencies and lockdown regulations on  $\text{NO}_2$  concentrations separate from meteorological influences. A prediction for  $\text{NO}_2$  VCDs over the NA could be made using the historical relations between meteorological parameters and TROPOMI measured anomalies (w.r.t. the 3-year mean) with a mean squared error of  $0.22 \text{ Pmolec/cm}^2$ . Dividing the weather-based prediction by the actual observed TROPOMI measurements, insight into the meteorological and anthropogenic contribution to retrieved  $\text{NO}_2$  VCDs was obtained (Figure 4.20). From analysis of the decision trees, major factors influencing the tropospheric column values were identified to be height of the troposphere, rain accumulation, wind, incoming shortwave radiation and temperature, consistent with literature (Falocchi et al. [2021], Yin et al. [2022]). Inherent to random forest modelling no quantitative relations are obtained between meteorological parameters and  $\text{NO}_2$  VCDs such that the results obtained here cannot easily be extrapolated to different spatio-temporal scenarios.

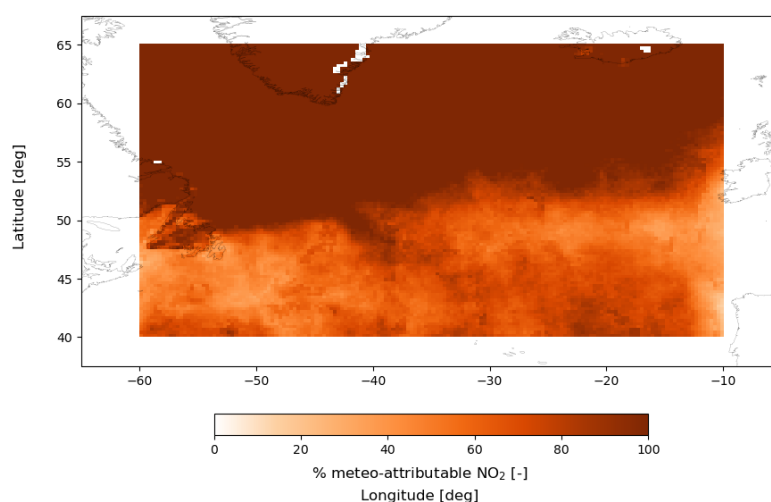


**Figure 4.20:** Average meteo-attributable contribution of measured  $\text{NO}_2$  VCDs

From Figure 4.20 can be deduced that a large part of the variation in tropospheric nitrogen dioxide could also be attributed to meteorology. At ( $64^\circ \text{ N}$ ,  $21^\circ \text{ W}$ ) a high source of non-meteorological attributable nitrogen dioxide can be identified. This could be attributed anthropogenic emissions as the location corresponds with the capital city of Iceland. Furthermore, below the  $50^\circ \text{ N}$  zonal band, larger percentages could not be attributed to meteorology. These could stem from anthropogenic shipping emissions which are likely to occur in that area (Figure 4.4). Another possible source of this contribution could be uncertainties in the TROPOMI retrievals, which in general are higher over areas with higher  $\text{NO}_2$  VCDs. An explanation for the in general high meteorology-attributable contribution of the measured  $\text{NO}_2$  VCDs may lie in the use of historical weather relations from MERRA-2 as uncertainties in reanalysis data and errors resulting from relations between meteorology at coarser resolution with TROPOMI measurements are introduced. Interesting research opportunities lie in the application of a chemistry transport model once meteorology input becomes available to retrieve more accurate background  $\text{NO}_2$  concentrations and meteorological contributions by simulating scenarios with and without aviation emission input.

# Bibliography

- D. J. Allen, K. E. Pickering, E. J. Bucsela, N. Krotkov, and R. Holzworth. Lightning NO<sub>x</sub> production in the tropics as determined using omi NO<sub>2</sub> retrievals and wvlln stroke data. *Journal of Geophysical Research: Atmospheres*, 124(23):13498–13518, 2019. doi: 10.1029/2019JD030561.
- D. J. Allen, K. E. Pickering, E. J. Bucsela, J. H. G. M. van Geffen, J. Lapierre, W. Koshak, and H. J. Eskes. Observations of lightning NO<sub>x</sub> production from tropospheric monitoring instrument case studies over the united states. *Journal of Geophysical Research: Atmospheres*, 126(10), 2021. doi: 10.1029/2020JD034174.
- V. Anh, H. Duc, and M. Azzi. Modeling anthropogenic trends in air quality data. *Journal of the Air & Waste Management Association*, 47(1):66–71, 1997. doi: 10.1080/10473289.1997.10464406.
- R. Atkinson. Atmospheric chemistry of vocs and no<sub>x</sub>. *Atmospheric environment*, 34(12-14):2063–2101, 2000. doi: 10.1016/S1352-2310(99)00460-4.
- J. Barré, H. Petetin, A. Colette, M. Guevara, V.-H. Peuch, L. Rouil, R. Engelen, A. Inness, J. Flemming, C. Pérez García-Pando, et al. Estimating lockdown-induced european no<sub>2</sub> changes using satellite and surface observations and air quality models. *Atmospheric chemistry and physics*, 21(9):7373–7394, 2021. doi: 10.5194/acp-21-7373-2021.
- S. R. H. Barrett, R. E. Britter, and I. A. Waitz. Global mortality attributable to aircraft cruise emissions. *Environmental Science and Technology*, 44:7736–7742, 10 2010. ISSN 0013936X. doi: 10.1021/es101325r.
- C. Bassani, F. Vichi, G. Esposito, M. Montagnoli, M. Giusto, and A. Ianniello. Nitrogen dioxide reductions from satellite and surface observations during COVID-19 mitigation in rome (italy). *Environmental Science and Pollution Research*, 28(18):22981–23004, 2021. doi: 10.1007/s11356-020-12141-9.
- S. L. Baughcum, T. G. Tritz, S. C. Henderson, and D. C. Pickett. Scheduled civil aircraft emission inventories for 1992: Database development and analysis. NASA CR-4700, 1996.
- M. Bauwens, S. Compennolle, T. Stavrou, J.-F. Müller, J. Van Gent, H. J. Eskes, P. F. Levelt, R. Van Der A, J. P. Veefkind, J. Vlietinck, et al. Impact of coronavirus outbreak on NO<sub>2</sub> pollution assessed using TROPOMI and omi observations. *Geophysical Research Letters*, 47(11), 2020. doi: 10.1029/2020GL087978.
- S. Beirle. *Estimating source strengths and lifetime of Nitrogen Oxides from satellite data*. PhD thesis, Heidelberg University, 2004.
- S. Beirle, U. Platt, R. Von Glasow, M. Wenig, and T. Wagner. Estimate of nitrogen oxide emissions from shipping by satellite remote sensing. *Geophysical Research Letters*, 31(18), 2004. doi: 10.1029/2004GL020312.
- J. D. Bradshaw, D. Davis, G. Grodzinsky, S. Smyth, R. Newell, S. Sandholm, and S. Liu. Observed distributions of nitrogen oxides in the remote free troposphere from the nasa global tropospheric experiment programs. *Reviews of Geophysics*, 38(1):61–116, 2000. doi: 10.1029/1999RG900015.
- E. J. Bucsela, K. E. Pickering, D. J. Allen, R. H. Holzworth, and N. A. Krotkov. Midlatitude lightning NO<sub>x</sub> production efficiency inferred from omi and wvlln data. *Journal of Geophysical Research: Atmospheres*, 124(23):13475–13497, 2019. doi: 10.1029/2018JD029824.
- E. J. Bucsela, K. E. Pickering, D. J. Allen, D. Loyola, H. J. Eskes, J. P. Veefkind, J. H. G. M. van Geffen, W. Koshak, and N. Krotkov. Improved lightning NO<sub>x</sub> production estimates using TROPOMI and glm data. In *AGU Fall Meeting Abstracts*, volume 2021, pages A24E–07, 2021.
- M. A. Cameron, M. Z. Jacobson, S. R. H. Barrett, H. Bian, C.-C. Chen, S. D. Eastham, A. Gettelman, A. Khodayari, Q. Liang, H. B. Selkirk, et al. An intercomparative study of the effects of aircraft emissions on surface air quality. *Journal of Geophysical Research: Atmospheres*, 122(15):8325–8344, 2017.

- K. L. Chan, E. Khorsandi, S. Liu, F. Baier, and P. Valks. Estimation of surface NO<sub>2</sub> concentrations over germany from TROPOMI satellite observations using a machine learning method. *Remote Sensing*, 13(5):969, 2021. doi: 10.3390/rs13050969.
- S. Choi, J. Joiner, Y. Choi, B. N. Duncan, A. Vasilkov, N. Krotkov, and E. J. Bucsela. First estimates of global free-tropospheric no<sub>2</sub> abundances derived using a cloud-slicing technique applied to satellite observations from the aura ozone monitoring instrument (omi). *Atmospheric Chemistry and Physics*, 14(19):10565–10588, 2014. doi: 10.5194/acp-14-10565-2014.
- M. J. Cooper, R. V. Martin, D. K. Henze, and D. B. A. Jones. Effects of a priori profile shape assumptions on comparisons between satellite NO<sub>2</sub> columns and model simulations. *Atmospheric Chemistry and Physics*, 20(12):7231–7241, 2020. doi: 10.5194/acp-20-7231-2020.
- Copernicus. Flawed estimates of the effects of lockdown measures on air quality derived from satellite observations, 2020. <https://atmosphere.copernicus.eu/flawed-estimates-effects-lockdown-measures-air-quality-derived-satellite-observations>, last visited 28-12-2022.
- M. A. G. Demetillo, A. Navarro, K. K. Knowles, K. P. Fields, J. A. Geddes, C. R. Nowlan, S. J. Janz, L. M. Judd, J. Al-Saadi, K. Sun, et al. Observing nitrogen dioxide air pollution inequality using high-spatial-resolution remote sensing measurements in houston, texas. *Environmental Science & Technology*, 54(16):9882–9895, 2020.
- W. Deng, J. B. Cohen, S. Wang, and C. Lin. Improving the understanding between climate variability and observed extremes of global NO<sub>2</sub> over the past 15 years. *Environmental Research Letters*, 16(5):054020, 2021.
- A. A. Donnelly, B. M. Broderick, and B. D. Misstear. The effect of long-range air mass transport pathways on pm<sub>10</sub> and NO<sub>2</sub> concentrations at urban and rural background sites in ireland: Quantification using clustering techniques. *Journal of Environmental Science and Health, Part A*, 50(7):647–658, 2015.
- EASA. Commission implementing regulation (EU) 2020/587 of 29 april 2020 amending implementing regulation (EU) no 1206/2011 laying down requirements on aircraft identification for surveillance for the single european sky and implementing regulation (EU) no 1207/2011 laying down requirements for the performance and the interoperability of surveillance for the single european sky. *Official Journal of the European Union - Legislation*, 32020R0587, 2020. [https://data.europa.eu/eli/reg\\_impl/2020/587/oj](https://data.europa.eu/eli/reg_impl/2020/587/oj), last visited 18-12-2022.
- S. Eckhardt, A. Stohl, S. Beirle, N. Spichtinger, P. James, C. Forster, C. Junker, T. Wagner, U. Platt, and S. G. Jennings. The north atlantic oscillation controls air pollution transport to the arctic. *Atmospheric Chemistry and Physics*, 3(5):1769–1778, 2003.
- H. J. Eskes and K. F. Boersma. Averaging kernels for DOAS total-column satellite retrievals. *Atmospheric Chemistry and Physics*, 3(5):1285–1291, 2003.
- H. J. Eskes, J. H. G. M. van Geffen, F. Boersma, K.-U. Eichmann, A. Apituley, M. Pedergnana, M. Sneep, J. P. Veefkind, and D. Loyola. Sentinel-5 precursor TROPOMI level 2 product user manual nitrogendioxide, technical report. (S5P-KNMI-L2-0021-MA), 2019.
- FAA. ATC transponder and altitude reporting equipment and use. *Code of Federal Regulations*, 91.215, 2019. <https://www.ecfr.gov/current/title-14/chapter-I/subchapter-F/part-91/subpart-C/section-91.215>, last visited 18-12-2022.
- M. Falocchi, D. Zardi, and L. Giovannini. Meteorological normalization of NO<sub>2</sub> concentrations in the province of bolzano (italian alps). *Atmospheric Environment*, 246:118048, 2021.
- D. Fowler, P. Brimblecombe, J. Burrows, M. R. Heal, P. Grennfelt, D. S. Stevenson, A. Jowett, E. Nemitz, M. Coyle, X. Liu, et al. A chronology of global air quality. *Philosophical Transactions of the Royal Society A*, 378(2183), 2020.



- R. Gelaro, W. McCarty, M. J. Suárez, R. Todling, A. Molod, L. Takacs, C. A. Randles, A. Darmenov, M. G. Bosilovich, R. Reichle, et al. The modern-era retrospective analysis for research and applications, version 2 (MERRA-2). *Journal of climate*, 30(14):5419–5454, 2017.
- A. K. Georgoulias, K. F. Boersma, J. V. Vliet, X. Zhang, R. V. D. A, Z. P, and J. D. Laet. Detection of NO<sub>2</sub> pollution plumes from individual ships with the TROPOMI/S5P satellite sensor. *Environmental Research Letters*, 15, 12 2020. ISSN 17489326. doi: 10.1088/1748-9326/abc445.
- D. L. Goldberg, S. C. Anenberg, D. Griffin, C. A. McLinden, Z. Lu, and D. G. Streets. Disentangling the impact of the COVID-19 lockdowns on urban NO<sub>2</sub> from natural variability. *Geophysical Research Letters*, 47(17):e2020GL089269, 2020.
- D. L. Goldberg, S. C. Anenberg, G. H. Kerr, A. Moheg, Z. Lu, and D. G. Streets. TROPOMI NO<sub>2</sub> in the united states: A detailed look at the annual averages, weekly cycles, effects of temperature, and correlation with surface NO<sub>2</sub> concentrations. *Earth's future*, 9(4):e2020EF001665, 2021.
- S. K. Grange, D. C. Carslaw, A. C. Lewis, E. Boleti, and C. Hueglin. Random forest meteorological normalisation models for swiss PM<sub>10</sub> trend analysis. *Atmospheric Chemistry and Physics*, 18(9): 6223–6239, 2018. doi: 10.5194/acp-18-6223-2018.
- D. Griffin, X. Zhao, C. A. McLinden, K. F. Boersma, A. Bourassa, E. Dammers, D. Degenstein, H. J. Eskes, L. Fehr, V. Fioletov, et al. High-resolution mapping of nitrogen dioxide with TROPOMI: First results and validation over the canadian oil sands. *Geophysical Research Letters*, 46(2):1049–1060, 2019.
- C. Grobler, P. J. Wolfe, K. Dasadhikari, I. C. Dedoussi, F. Allroggen, R. L. Speth, S. D. Eastham, A. Agarwal, M. Staples, J. Sabnis, and S. R. H. Barrett. Marginal climate and air quality costs of aviation emissions. *Environmental Research Letters*, 14, 2019. ISSN 17489326. doi: 10.1088/1748-9326/ab4942.
- HCON. Health council of the netherlands, dutch expert committee on occupational standards. nitrogen dioxide; health-based recommended occupational exposure limit, 2004. Publication no. 2004/01OSH.
- S. C. Herndon, J. H. Shorter, M. S. Zahniser, D. D. Nelson, J. J. Wormhoudt, R. C. Miake-Lye, I. Waitz, P. Silva, T. Lanni, K. Demerjian, and C. E. Kolb. NO and NO<sub>2</sub> emission ratios measured from in use commercial aircraft during taxi and take-off. *Environmental Science Technology*, 38,22:6078–6084, 10 2004. doi: 10.1021/es049701c.
- R. M. Hoesly, S. J. Smith, L. Feng, Z. Klimont, G. Janssens-Maenhout, T. Pitkanen, J. J. Seibert, L. Vu, R. J. Andres, R. M. Bolt, T. C. Bond, L. Dawidowski, N. Kholod, J.-I. Kurokawa, M. Li, L. Liu, Z. Lu, M. C. P. Moura, P. R. O'Rourke, and Q. Zhang. Historical (1750–2014) anthropogenic emissions of reactive gases and aerosols from the community emissions data system (ceds). *Geoscientific Model Development*, 11(1):369–408, 2018. doi: 10.5194/gmd-11-369-2018.
- I. Ialongo, H. Virta, H. J. Eskes, J. Hovila, and J. Douros. Comparison of TROPOMI/sentinel-5 precursor NO<sub>2</sub> observations with ground-based measurements in helsinki. *Atmospheric Measurement Techniques*, 13(1):205–218, 2020.
- M. Z. Jacobson, J. T. Wilkerson, A. D. Naiman, and S. K. Lele. The effects of aircraft on climate and pollution. part ii: 20-year impacts of exhaust from all commercial aircraft worldwide treated individually at the subgrid scale. *Faraday Discussions*, 165:369–382, 2013.
- M. Kampa and E. Castanas. Human health effects of air pollution. *Environmental pollution (Barking, Essex : 1987)*, 151:362–7, 02 2008. doi: 10.1016/j.envpol.2007.06.012.
- K. D. Kanniah, N. A. F. K. Zaman, and K. Perumal. Analysis of NO<sub>2</sub> tropospheric column amount at airports in malaysia before and during COVID-19 pandemic using sentinel-5p TROPOMI data. volume 43, pages 399–403. International Society for Photogrammetry and Remote Sensing, 6 2021. doi: 10.5194/isprs-archives-XLIII-B3-2021-399-2021.

- B. Y. Kim, G. G. Fleming, J. J. Lee, I. A. Waitz, J.-P. Clarke, S. Balasubramanian, A. Malwitz, K. Klima, M. Locke, C. A. Holsclaw, L. Q. Maurice, and M. L. Gupta. System for assessing aviation's global emissions (SAGE), part 1: Model description and inventory results. *Transportation Research Part D: Transport and Environment*, 12(5):325–346, 2007. ISSN 1361-9209. doi: 10.1016/j.trd.2007.03.007.
- M.-E. Koukoulis, I. Skoulidou, A. Karavias, I. Parcharidis, D. Balis, A. Manders, A. Segers, H. J. Eskes, and J. H. G. M. van Geffen. Sudden changes in nitrogen dioxide emissions over Greece due to lockdown after the outbreak of COVID-19. *Atmospheric Chemistry and Physics*, 21(3):1759–1774, 2021. doi: 10.5194/acp-21-1759-2021.
- S. Kurchaba, J. van Vliet, F. J. Verbeek, J. J. Meulman, and C. J. Veenman. Supervised segmentation of NO<sub>2</sub> plumes from individual ships using TROPOMI satellite data. *arXiv preprint arXiv:2203.06993*, 2022.
- L. N. Lamsal, R. V. Martin, E. A. Van Donkelaar, A. Celarier, E. J. Bucsela, K. F. Boersma, R. Dirksen, C. Luo, and Y. Wang. Indirect validation of tropospheric nitrogen dioxide retrieved from the OMI satellite instrument: Insight into the seasonal variation of nitrogen oxides at northern midlatitudes. *Journal of Geophysical Research: Atmospheres*, 115(D5), 2010.
- A. S. Lawal, A. G. Russell, and J. Kaiser. Assessment of airport-related emissions and their impact on air quality in Atlanta, GA, using CMAQ and TROPOMI. *Environmental Science and Technology*, 56:98–108, 1 2022. ISSN 15205851. doi: 10.1021/acs.est.1c03388.
- D. S. Lee, B. Brunner, A. Döpelheuer, R. S. Falk, R. M. Gardner, M. Lecht, M. Leech, D. H. Lister, and P. J. Newton. Aviation emissions: Present-day and future. *Meteorologische Zeitschrift*, 11:141–150, 05 2002. doi: 10.1127/0941-2948/2002/0011-0141.
- H. Lee, S. C. Olsen, D. J. Wuebbles, and D. Youn. Impacts of aircraft emissions on the air quality near the ground. *Atmospheric Chemistry and Physics*, 13(11):5505–5522, 2013.
- J. Lelieveld, J. S. Evans, M. Fnais, D. Giannadaki, and A. Pozzer. The contribution of outdoor air pollution sources to premature mortality on a global scale. *Nature*, 525:367–371, 9 2015. ISSN 14764687. doi: 10.1038/nature15371. contribution of outdoor pollution to mortality, mostly PM<sub>2.5</sub> but some examples of.
- S. Long, X. Wei, F. Zhang, R. Zhang, J. Xu, K. Wu, Q. Li, and W. Li. Estimating daily ground-level NO<sub>2</sub> concentrations over China based on TROPOMI observations and machine learning approach. *Atmospheric Environment*, 289:119310, 2022.
- A. Lorente, K. F. Boersma, H. J. Eskes, J. P. Veefkind, J. H. G. M. van Geffen, M. B. De Zeeuw, H. A. C. Denier Van Der Gon, S. Beirle, and M. C. Krol. Quantification of nitrogen oxides emissions from build-up of pollution over Paris with TROPOMI. *Scientific reports*, 9(1):1–10, 2019.
- I. Manisalidis, E. Stavropoulou, A. Stavropoulos, and E. Bezirtzoglou. Environmental and health impacts of air pollution: A review. *Frontiers in Public Health*, 8, 2020. ISSN 2296-2565. doi: 10.3389/fpubh.2020.00014.
- E. A. Marais, J. F. Roberts, R. G. Ryan, H. J. Eskes, K. F. Boersma, S. Choi, J. Joiner, N. Abuhassan, A. Redondas, M. Grutter, et al. New observations of NO<sub>2</sub> in the upper troposphere from TROPOMI. *Atmospheric Measurement Techniques*, 14(3):2389–2408, 2021.
- M. Masiol and R. Harrison. Aircraft engine exhaust emissions and other airport-related contributions to ambient air pollution: A review. *Atmospheric Environment*, 95:409–455, 05 2014. doi: 10.1016/j.atmosenv.2014.05.070.
- T. F. Mentel, D. Bleilbens, and A. Wahner. A study of nighttime nitrogen oxide oxidation in a large reaction chamber—the fate of NO<sub>2</sub>, N<sub>2</sub>O<sub>5</sub>, HNO<sub>3</sub>, and O<sub>3</sub> at different humidities. *Atmospheric Environment*, 30(23):4007–4020, 1996.
- H. Morita, S. Yang, N. Unger, and P. L. Kinney. Global health impacts of future aviation emissions under alternative control scenarios. *Environmental Science & Technology*, 48(24):14659–14667, 2014.



- V. Mouillet. User manual for the base of aircraft data (bada) revision 3.14. *EUROCONTROL Exp. Centre, Brétigny, France, Tech. Rep.*, 17(05):29–143, 2017.
- T. Nishanth, K. M. Praseed, and M. K. Kumar. Solar eclipse-induced variations in solar flux, j (NO<sub>2</sub>) and surface ozone at kannur, india. *Meteorology and Atmospheric Physics*, 113(1):67–73, 2011.
- F. Pedregosa, G. Varoquaux, A. Gramfort, V. Michel, B. Thirion, O. Grisel, M. Blondel, P. Prettenhofer, R. Weiss, V. Dubourg, et al. Scikit-learn: Machine learning in python. *the Journal of machine Learning research*, 12:2825–2830, 2011.
- F. J. Pérez-Invernón, H. Huntrieser, T. Erbertseder, D. Loyola, P. Valks, S. Liu, D. J. Allen, K. E. Pickering, E. J. Bucsela, P. Jöckel, et al. Quantification of lightning-produced no<sub>x</sub> over the pyrenees and the ebro valley by using different TROPOMI-no<sub>2</sub> and cloud research products. *Atmospheric Measurement Techniques*, 15(11):3329–3351, 2022.
- K. E. Pickering, E. Bucsela, D. Allen, A. Ring, R. Holzworth, and N. Krotkov. Estimates of lightning NO<sub>x</sub> production based on omi NO<sub>2</sub> observations over the gulf of mexico. *Journal of Geophysical Research: Atmospheres*, 121(14):8668–8691, 2016.
- K. Qin, L. Rao, J. Xu, Y. Bai, J. Zou, N. Hao, S. Li, and C. Yu. Estimating ground level NO<sub>2</sub> concentrations over central-eastern china using a satellite-based geographically and temporally weighted regression model. *Remote Sensing*, 9(9):950, 2017.
- F. D. Quadros, M. Snellen, and I. C. Dedoussi. Recent and projected trends in global civil aviation fleet average NO<sub>x</sub> emissions indices. In *AIAA Scitech 2022 Forum*, page 2051, 2022a. doi: 10.2514/6.2022-2051.
- F. D. A. Quadros, M. Snellen, J. Sun, and I. C. Dedoussi. Global civil aviation emissions estimates for 2017–2020 using ads-b data. *Journal of Aircraft*, pages 1–11, 2022b.
- A. Richter, V. Eyring, J. P. Burrows, H. Bovensmann, A. Lauer, B. Sierk, and P. J. Crutzen. Satellite measurements of NO<sub>2</sub> from international shipping emissions. *Geophysical Research Letters*, 31(23), 2004.
- M. Schaefer, M. Jung, and H. Pabst. The regional distribution of air traffic emissions in the past, present and future, 2013.
- U. Schumann, H. Schlager, F. Arnold, J. Ovarlez, H. Kelder, Ø. Hov, G. Hayman, I. Isaksen, J. Staehelin, and P. D. Whitefield. Pollution from aircraft emissions in the north atlantic flight corridor: Overview on the polinat projects. *Journal of Geophysical Research: Atmospheres*, 105(D3):3605–3631, 2000.
- J. H. Seinfeld and S. N. Pandis. *Atmospheric chemistry and physics: From air pollution to climate change, second edition*. John Wiley & Sons, New York, 2006.
- X. Shi and G. P. Brasseur. The response in air quality to the reduction of chinese economic activities during the COVID-19 outbreak. *Geophysical Research Letters*, 47(11), 2020. doi: 10.1029/2020GL088070.
- L. Shikwambana and M. Kganyago. Assessing the responses of aviation-related so<sub>2</sub> and NO<sub>2</sub> emissions to COVID-19 lockdown regulations in south africa. *Remote Sensing*, 13, 10 2021. ISSN 20724292. doi: 10.3390/rs13204156.
- R. F. Silvern, D. J. Jacob, L. J. Mickley, M. P. Sulprizio, K. R. Travis, E. A. Marais, R. C. Cohen, J. L. Laughner, S. Choi, J. Joiner, and L. N. Lamsal. Using satellite observations of tropospheric no<sub>2</sub> columns to infer long-term trends in us NO<sub>x</sub> emissions: the importance of accounting for the free tropospheric NO<sub>2</sub> background. *Atmospheric Chemistry and Physics*, 19(13):8863–8878, 2019. doi: 10.5194/acp-19-8863-2019.
- S. J. Smith, Y. Zhou, P. Kyle, H. Wang, and H. Yu. A community emissions data system (ceds): emissions for cmip6 and beyond. In *Proceedings of the 2015 International Emission Inventory Conference, San Diego, CA, USA*, pages 12–16, 2015.

- N. Spichtinger, M. Wenig, P. James, T. Wagner, U. Platt, and A. Stohl. Satellite detection of a continental-scale plume of nitrogen oxides from boreal forest fires. *Geophysical Research Letters*, 28(24):4579–4582, 2001.
- T. Stavrou, J.-F. Müller, K. F. Boersma, R. J. Van Der A, J. Kurokawa, T. Ohara, and Q. Zhang. Key chemical  $\text{NO}_x$  sink uncertainties and how they influence top-down emissions of nitrogen oxides. *Atmospheric Chemistry and Physics*, 13(17):9057–9082, 2013.
- M. E. J. Stettler, S. Eastham, and S. R. H. Barrett. Air quality and public health impacts of uk airports. part i: Emissions. *Atmospheric Environment*, 45:5415–5424, 10 2011. doi: 10.1016/j.atmosenv.2011.07.012.
- A. Stohl, H. Huntrieser, A. Richter, S. Beirle, O. R. Cooper, S. Eckhardt, C. Forster, P. James, N. Spichtinger, M. Wenig, et al. Rapid intercontinental air pollution transport associated with a meteorological bomb. *Atmospheric Chemistry and Physics*, 3(4):969–985, 2003.
- M. Strohmeier, X. Olive, J. Lübke, M. Schäfer, and V. Lenders. Crowdsourced air traffic data from the opensky network 2019–2020. *Earth System Science Data*, 13(2), 2021. doi: 10.5194/essd-13-357-2021.
- K. N. Tait, M. A. H. Khan, S. Bullock, M. H. Lowenberg, and D. E. Shallcross. Aircraft emissions, their plume-scale effects, and the spatio-temporal sensitivity of the atmospheric response: A review. *Aerospace*, 9(7):355, 2022.
- L. Tarrasón, J. E. Jonson, T. K. Berntsen, and K. Rypdal. Study on air quality impacts of non-Ito emissions from aviation. *Norwegian Meteorological Institute*, 2004. Technical report 3, Report to the european committee under contract B4-30402002343093MARC1.
- K. R. Travis, D. J. Jacob, J. A. Fisher, P. S. Kim, E. A. Marais, L. Zhu, K. Yu, C. C. Miller, R. M. Yantosca, M. P. Sulprizio, et al. Why do models overestimate surface ozone in the southeast united states? *Atmospheric Chemistry and Physics*, 16(21):13561–13577, 2016.
- J. H. G. M. van Geffen, K. F. Boersma, H. J. Eskes, M. Sneep, T. Linden, M. Zara, and J. P. Veefkind. S5P TROPOMI  $\text{NO}_2$  slant column retrieval: Method, stability, uncertainties and comparisons with omi. *Atmospheric Measurement Techniques*, 2020.
- J. H. G. M. van Geffen, H. J. Eskes, K. F. Boersma, , and J. P. Veefkind. TROPOMI atbd of the total and tropospheric  $\text{NO}_2$  data products, report s5p-knmi-l2-0005-rp. 2022a. <http://www.{TROPOMI}.eu/data-products/nitrogen-dioxide>, last visited 17-11-2022.
- J. H. G. M. van Geffen, H. J. Eskes, S. Compennolle, G. Pinardi, T. Verhoelst, J.-C. Lambert, M. Sneep, M. Ter Linden, A. Ludewig, K. F. Boersma, et al. Sentinel-5p TROPOMI no 2 retrieval: impact of version v2. 2 improvements and comparisons with omi and ground-based data. *Atmospheric Measurement Techniques*, 15(7):2037–2060, 2022b.
- J. P. Veefkind, I. Aben, K. McMullan, H. Förster, J. De Vries, G. Otter, J. Claas, H. J. Eskes, J. F. De Haan, Q. Kleipool, et al. Tropomi on the esa sentinel-5 precursor: A gmes mission for global observations of the atmospheric composition for climate, air quality and ozone layer applications. *Remote sensing of environment*, 120:70–83, 2012.
- T. Verhoelst, S. Compennolle, G. Pinardi, J.-C. Lambert, H. J. Eskes, K.-U. Eichmann, A. M. Fjæraa, J. Granville, S. Niemeijer, A. Cede, M. Tiefengraber, F. Hendrick, A. Pazmiño, A. Bais, A. Bazureau, K. F. Boersma, K. Bogner, A. Dehn, S. Donner, A. Elokho, M. Gebetsberger, F. Goutail, M. Grutter de la Mora, A. Gruzdev, M. Gratsea, G. H. Hansen, H. Irie, N. Jepsen, Y. Kanaya, D. Karagiorgidis, R. Kivi, K. Kreher, P. F. Levelt, C. Liu, M. Müller, M. Navarro Comas, A. J. M. Pijters, J.-P. Pommereau, T. Portafaix, C. Prados-Roman, O. Puentedura, R. Querel, J. Remmers, A. Richter, J. Rimmer, C. Rivera Cárdenas, L. Saavedra de Miguel, V. P. Sinyakov, W. Stremme, K. Strong, M. Van Roozendael, J. P. Veefkind, T. Wagner, F. Wittrock, M. Yela González, and C. Zehner. Ground-based validation of the copernicus sentinel-5p TROPOMI  $\text{NO}_2$  measurements with the ndacc zsl-doas, max-doas and pandonia global networks. *Atmospheric Measurement Techniques*, 14(1):481–510, 2021. doi: 10.5194/amt-14-481-2021.

- M. Vîrghileanu, I. Săvulescu, B.-A. Mihai, C. Nistor, and R. Dobre. Nitrogen dioxide (NO<sub>2</sub>) pollution monitoring with sentinel-5p satellite imagery over europe during the coronavirus pandemic outbreak. *Remote Sensing*, 12(21):3575, 2020.
- T. V. Vu, Z. Shi, J. Cheng, Q. Zhang, K. He, S. Wang, and R. M. Harrison. Assessing the impact of clean air action on air quality trends in beijing using a machine learning technique. *Atmospheric Chemistry and Physics*, 19(17):11303–11314, 2019.
- T. Wang, J. Shi, Y. Ma, L. Husi, E. Comyn-Platt, D. Ji, T. Zhao, and C. Xiong. Recovering land surface temperature under cloudy skies considering the solar-cloud-satellite geometry: Application to modis and landsat-8 data. *Journal of Geophysical Research: Atmospheres*, 124(6):3401–3416, 2019.
- J. T. Wilkerson, M. Z. Jacobson, A. Malwitz, S. Balasubramanian, R. Wayson, G. Fleming, A. D. Naiman, and S. K. Lele. Analysis of emission data from global commercial aviation: 2004 and 2006. *Atmospheric Chemistry and Physics*, 10:6391–6408, 2010. ISSN 16807316. doi: 10.5194/acp-10-6391-2010.
- J. E. Williams, K. F. Boersma, P. Le Sager, and W. W. Verstraeten. The high-resolution version of tm5-mp for optimized satellite retrievals: description and validation. *Geoscientific Model Development*, 10(2):721–750, 2017.
- J. Wormhoudt, S. C. Herndon, P. E. Yelvington, R. C. Miake-Lye, and C. Wey. Nitrogen oxide (no/no<sub>2</sub>/hono) emissions measurements in aircraft exhausts. *Journal of Propulsion and Power*, 23(5):906–911, 2007.
- Q. Wu, T. Li, S. Zhang, J. Fu, B. C. Seyler, Z. Zhou, X. Deng, B. Wang, and Y. Zhan. Evaluation of NO<sub>x</sub> emissions before, during, and after the COVID-19 lockdowns in china: A comparison of meteorological normalization methods. *Atmospheric Environment*, 278:119083, 2022.
- S. H. L. Yim, G. L. Lee, I. H. Lee, F. Allroggen, A. Ashok, F. Caiazzo, S. Eastham, R. Malina, and S. R. H. Barrett. Global, regional and local health impacts of civil aviation emissions. *Environmental Research Letters*, 10, 3 2015. ISSN 17489326. doi: 10.1088/1748-9326/10/3/034001.
- H. Yin, Y. Sun, J. Notholt, M. Palm, and C. Liu. Spaceborne tropospheric nitrogen dioxide (no<sub>2</sub>) observations from 2005–2020 over the yangtze river delta (yrd), china: variabilities, implications, and drivers. *Atmospheric Chemistry and Physics*, 22(6):4167–4185, 2022.
- X. Zhang, Y. Yin, R. van der A, J. L. Lapierre, Q. Chen, X. Kuang, S. Yan, J. Chen, C. He, and R. Shi. Estimates of lightning no<sub>x</sub> production based on high-resolution omi no<sub>2</sub> retrievals over the continental us. *Atmospheric Measurement Techniques*, 13(4):1709–1734, 2020.
- Y. Zhang, H. Bo, Z. Jiang, Y. Wang, Y. Fu, B. Cao, X. Wang, J. Chen, and R. Li. Untangling the contributions of meteorological conditions and human mobility to tropospheric NO<sub>2</sub> in Chinese mainland during the COVID-19 pandemic in early 2020. *National Science Review*, 8(11), 04 2021. ISSN 2095-5138. doi: 10.1093/nsr/nwab061.
- X. Zhao, D. Griffin, V. Fioletov, C. McLinden, A. Cede, M. Tiefengraber, M. Müller, K. Bognar, K. Strong, F. Boersma, H. J. Eskes, J. Davies, A. Ogyu, and S. C. Lee. Assessment of the quality of TROPOMI high-spatial-resolution NO<sub>2</sub> data products in the greater toronto area. *Atmospheric Measurement Techniques*, 13(4):2131–2159, 2020. doi: 10.5194/amt-13-2131-2020.
- H. Ziereis, H. Schlager, P. Schulte, P. F. J. Van Velthoven, and F. Slemr. Distributions of no, no<sub>x</sub>, and no<sub>y</sub> in the upper troposphere and lower stratosphere between 28 and 61 n during polinat 2. *Journal of Geophysical Research: Atmospheres*, 105(D3):3653–3664, 2000.